Waking Experience and Circadian Rhythms Result in Differential Modulation of Sleep and Wake States

Waking Experience and Circadian Rhythms Result in Differential Modulation of Sleep and Wake States

Amelia Hidalgo

A Thesis in the Field of Biotechnology

for the Degree of Master of Liberal Arts in Extension Studies

Harvard University

November 2021

Abstract

Sleep is thought to be tightly regulated by two processes, a homeostatic and a circadian process, which interact in a complex way to integrate prior wakefulness and circadian time (Borbély et al., 1982). Despite extensive research, however, little is known about how each contributes to the regulation of sleep and wake states. The goal of this study was to explore the regulation of sleep and wake during and after extended wakefulness and describe how different waking experiences may contribute to changes in brain-wide electrophysiological activity and neuronal activity reporters. In addition, sleep and wake regulation was compared in the presence and absence of circadian rhythms. This study demonstrates that waking experience during sleep deprivation (SD) changes sleep state dynamics following SD and results in experience-specific electroencephalography (EEG) patterns during wake. Sleep and wake regulation was shown to be different in rhythmic and arrhythmic animals. This difference was reflected in the percent of time spent in each state and in cumulative amounts of slow wave sleep (SWS) and rapid-eye movement (REM) sleep at baseline and during and after sleep deprivation. An automated pipeline for detecting whole brain neuronal activity reporters in 2D sections was also developed as a complement to EEG studies, allowing for the interrogation of changes in regional activity over time. Taken together, this study contributes to our understanding of sleep-wake regulation by demonstrating (1) that wake experiences differentially modulate sleep homeostatic responses and (2) that the

homeostat responds differently to high sleep pressure in the absence of circadian rhythms.

Dedication

To Corinne, Bertha and Hilario

Acknowledgments

This thesis would not have been possible without the support and guidance of many people and groups of people in my life. First of all, I'd like to thank the faculty and staff at Harvard Extension School who have made this master's degree possible. To have been able to get an advanced degree while working full time is a privilege and I am so grateful. Thank you to my academic and research advisors, Joan Short and James Morris, for guiding me through this process and helping me figure out how to juggle the last stretch of my master's in the midst of a move to Switzerland and a global pandemic. Thank you also to the support and administrative staff of the Biozentrum at the University of Basel, especially Alexandra Eberhardt and Manuela Holzer, for making my move abroad as painless as possible and for fielding my many questions.

Many thanks to my thesis director, Alexander Schier, for all of his guidance, support and encouragement. Thank you for creating a lab environment which fosters collaboration, open communication and scientific creativity. From personal experience, I know this kind of environment is unique and not easily found. I am so grateful to be a part of this "artist colony" and to have been provided with opportunities I could never have imagined. To my fellow Schier lab members (past and present), I am grateful to be among so many talented individuals such as yourselves. Your intelligence, kindness and passion for science is truly an inspiration.

A very special thank you goes out to two particular Schier lab members. I'd like to express my deepest gratitude and appreciation to Vassilis Bitsikas and William Joo.

They have been my mentors and colleagues for several years now. Their joint project on sleep homeostasis served as the inspiration and jumping off point for this thesis. Vassilis and Will, you are two of the most hard-working, driven and intelligent people I know. I am in awe of all that you do. Your never-ending patience, understanding and support has been so appreciated. Thank you doesn't even begin to cover it - but thank you for believing in my potential and for challenging me to be the best I can be. I've learned many things about life and science through you.

Lastly, I want to thank my family. To my mother and grandmother, Corinne and Bertha Hidalgo, you have been examples throughout my life of what I have most wanted to be –strong, independent women. The sacrifices you have made for me and the constant love, faith and support you have shown during both good and bad times is what has gotten me to where I am. I'd also like to acknowledge and thank my grandfather, who, although no longer with us, sparked my interest in neuroscience and set me on this path of scientific inquiry.

Table of Contents

List of Figures

Chapter I.

Introduction

Sleep is a heavily regulated state of high physiological importance; however, little is known about the mechanisms underlying its homeostatic control. A complex network of neuronal populations has been implicated in the production and regulation of sleep and wake states. These regions continuously interact, taking into account circadian rhythms and the amount of prior wake and/or sleep. Accompanying changes in regional activity leads to state-specific EEG patterns. These patterns provide insight into the homeostatic regulation of arousal and sleep states. This work aims to explore the regulation of sleep and wake during and after extended wakefulness and describe how different waking experiences may contribute to changes in brain-wide activity. Patterns present in animals with and without intact circadian rhythms will be compared and a tool presented which enables whole brain quantification of regional activity in two-dimensional sections.

Characterization and Function of the Sleep and Wake States

Sleep or sleep-like states have been observed in all animal species studied to date. From an evolutionary perspective, this conservation suggests that sleep plays an essential role in survival. Unfortunately, unlike other necessities such as food and water, sleep's function is not so easily understood. Its importance, however, has been highlighted by research in vertebrates and invertebrates alike. A seminal study performed

in rats demonstrated that sleep is necessary for survival. Rats that were prevented from sleeping at all developed a debilitated appearance, severe skin lesions and rapid weight loss despite increased eating. All animals died within 11 to 32 days (Rechtschaffen et al., 1989). Although this study suggests that severe sleep deprivation decreases survival, it is unknown whether this is due to sleep deprivation alone or is secondary to the high levels of stress caused by it. Extensive research has also demonstrated that sleep is critical for proper immune function and learning and memory, among other physiological processes. Following varying amounts of sleep deprivation, both humans and animals display weakened immune responses and worsened memory consolidation (Feld et al., 2017; Irwin and Opp, 2017).

Sleep can be defined behaviorally and via the use of electroencephalography (EEG) and electromyography (EMG). Behavioral criteria for sleep include, but are not limited to, loss of locomotor activity, maintenance of species-specific posture, rapid reversibility, increased threshold for response to external stimuli, and homeostatic rebound following sleep deprivation (Hayashi et al, 2017; Zimmerman et al., 2008). EEG and EMG can be used to detect brain cortical and skeletal muscle electrical activity, respectively, with each state having distinct electrophysiological properties.

Based on EEG and EMG data, wake is characterized by low amplitude, high frequency gamma oscillations (30-80 Hz) and high muscle tone (Weber and Dan 2016). Oscillations in this gamma range have been widely studied due to their association with sensory processing, learning, memory and focused attention (Cardin, 2016). While wake is traditionally classified as one state, sleep in mammals is divided into two main stages: rapid eye movement (REM) and non-rapid eye movement (NREM) sleep. Upon sleep

onset, mammals enter into NREM sleep. NREM sleep in rodents is considered a single state characterized by low frequency, high amplitude neuronal oscillations (0.5-4.5 Hz) in addition to a progressive decrease in muscle tone (Weber and Dan, 2016) (Figure 1). It is often commonly referred to as deep sleep. NREM sleep is often followed by REM sleep, which exhibits high frequency, low amplitude oscillations similar to wake (5-9 Hz) but is distinguished from it by a complete loss of muscle tone (Weber and Dan, 2016; Katsageorgiou et al., 2018) (Figure 1). Due to the simultaneous occurrence of these characteristics, this state is also known as paradoxical sleep. A higher arousal threshold is seen in REM sleep, making arousal more difficult and resulting in grogginess if interrupted. REM is commonly associated with dreaming in humans; however, recent studies have demonstrated dreams can also occur in NREM sleep (Siclari et al., 2018).

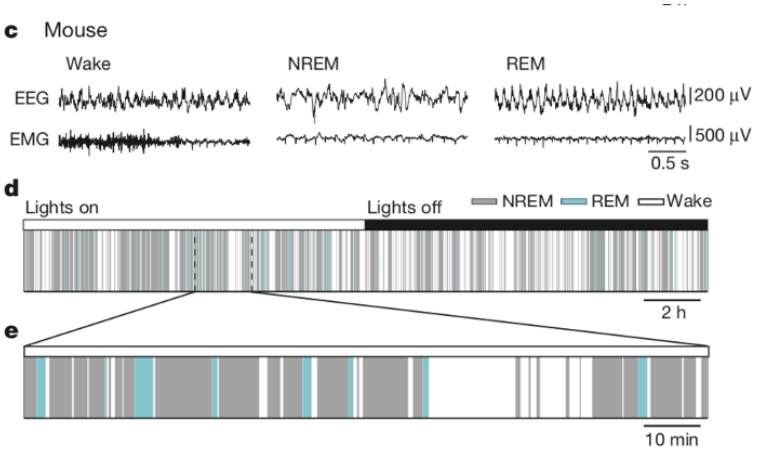

Figure 1: Schematic of EEG and EMG activity during sleep and arousal.
Upper: Example EEG and EMG from a mouse during wake, NREM and REM. Lower: Distribution of each state of a 24-hour period. (Adapted from Weber and Dan, 2016)

Sleep Regulation and Homeostasis

Over the course of wakefulness, one begins to feel tired and experiences an

increasingly strong urge (or drive) to fall asleep, resulting from the development of a sleep deficit. This deficit is thought to be restored during sleep, returning the body back to a state of homeostasis. Given the conserved nature of sleep and wake states across animal species, the drive to fall asleep and how sleep itself is regulated have been the subject of significant research. In 1982, Alexander Borbely put forth the influential idea that sleep is regulated by two distinct processes. This model proposes that the interaction of a sleep-dependent process (Process S) and a sleep-independent process (Process C) determines important aspects of sleep regulation (Borbely 1982, 2016).

Process S, derived from electrophysiological data showing changes in EEG frequencies over time, is meant to mimic the homeostatic process. The amount of slow wave activity (SWA) (0.5-4.0 Hz), a characteristic of NREM sleep, increases at the start of sleep and dissipates prior to awakening. Following sleep deprivation, the power density of SWA is increased relative to baseline (Figure 2). These lines of evidence suggest that SWA correlates with the amount of prior wakefulness and, therefore, reflects sleep pressure. According to the model, S triggers sleep at its peak (high sleep pressure) and triggers wake at its lowest boundary (low sleep pressure).

The second process regulating sleep homeostasis, Process C, mimics processes controlled by a circadian oscillator (Figure 2). Core body temperature (CBT) is one of the key markers of C (Borbely et al., 2016). CBT follows a nearly sinusoidal rhythm over the course of the day, a periodicity which is closely mimicked by sleep propensity (Lack et al., 2008). Sleep initiation typically occurs during the falling limb of CBT's trajectory, with the highest sleep propensity occurring when body temperature is lowest (Lack et al., 2008; Borbely et al., 1982). This same trend is seen even in the absence of external cues

such as light. Being able to study sleep without the influence of external entrainment cues is important in dissecting the influence of circadian timing. The organization of sleep has particular patterns with and without entrainment. REM sleep has a strong circadian aspect to it, displaying an inverse relationship with body temperature. With entrainment, REM sleep propensity is highest when CBT is at its minimum. In non-entrained conditions, there is either no rise in REM propensity or a decrease is seen (Borbely et al., 1982).

Process S and Process C continuously interact. Borbely's two-process model posits that sleep occurs as Process S reaches its upper bound and that wake is more likely to occur when S reaches its lower threshold. This corresponds to the descending and ascending limb of Process C, respectively. Sleep propensity is considered to be a function of the distance between S and C at any given point. Therefore, when the bounds of S and C are close together, sleep propensity is low. Conversely, if there is a large distance between the two, sleep propensity is high. During sleep deprivation, Process S can be extended. Theoretically this creates a greater difference between the two processes, resulting in higher sleep propensity relative to baseline. In Borbely's original 1982 model, Process S was believed to not influence Process C. Since then, Borbely has proposed an updated version, stating that high sleep pressure can decrease the amplitude of the circadian component. It then follows that low sleep pressure increases the amplitude of Process C (Borbely et al., 2016). Although Process S and Process C continuously interact, they are regulated by distinct processes. This independent regulation has been demonstrated in studies showing that animals rendered arrhythmic by lesions to the SCN did not have disrupted sleep homeostasis (Toblet et al., 1983; Trachsel et al., 1992).

A more recent model, the synaptic homeostasis hypothesis, builds off of Borbely's work by positing that Process S is actually displaying the increase in total synaptic strength over the course of wakefulness and its subsequent decrease, or downscaling, during sleep (Figure 3). The model states that during wake, interactions with the environment result in the acquisition of information about it, which is stored via long-term potentiation of synaptic strength. This net increase in synaptic strength leads to increased energy and space requirements in the brain and contributes to learning saturation. Upon sleep onset, we become less connected and responsive to our environment, providing an opportunity to decrease this burden and return to a baseline state. Changes in neuromodulatory milieu in response to stimuli over the course of wake and increased synaptic strength results in highly synchronized neuronal activity during early sleep. This activity is seen as slow waves of high amplitude, or SWA (Tononi & Cirelli, 2006).

Slow waves in NREM sleep are known to reflect changes in resting membrane potentials of neurons in the cortex and thalamus. Neurons that are depolarized are termed to be in an 'UP' state, while depolarized neurons are in a 'DOWN' state (Adamantidis et al., 2019). The synaptic homeostasis hypothesis states that periods of depolarization and hyperpolarization during sleep result in a proportional downscaling of synapses. This leads to a decrease in total synaptic strength and reduces the amplitude and synchronization of SWA over time. Synaptic downscaling allows for the efficient integration of information acquired during wake, while preventing the overload of neural circuitry and resources. The result of this process is the ability to begin this cycle anew upon wake. Evidence for this model is largely founded in experiments demonstrating the

increase of LTP-related genes and synaptic density during both spontaneous wakefulness and sleep deprivation. In contrast, LTP markers are severely diminished or abolished during sleep (Cirelli et al., 2004). Prolonged wakefulness by gentle handling has been found to increase the expression of synaptic potentiation markers in wake followed by an increase in SWA during sleep (Cirelli et al., 1996). Reduction in the expression of LTP-related genes in the cerebral cortex following wake led to a lower peak in SWA compared to baseline (Cirelli et al., 2005).

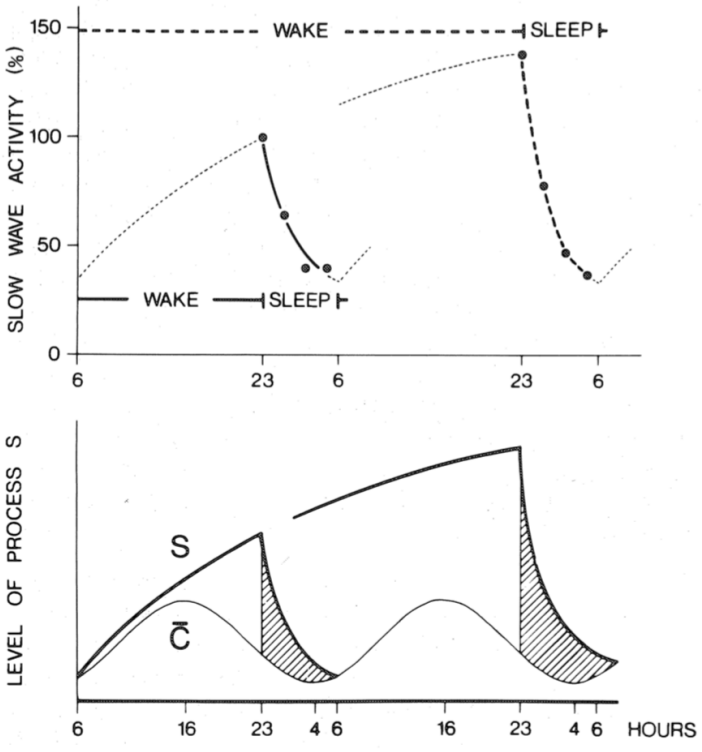

Figure 2: Two process model of sleep regulation.
Upper: The exponential decrease in SWA over the course of sleep and increase over baseline (100%) following extended wakefulness. Lower: The relationship between Process S and Process C over a 24 hour period at baseline and following extended wake. (Borbely, 1982 Figure 4.)

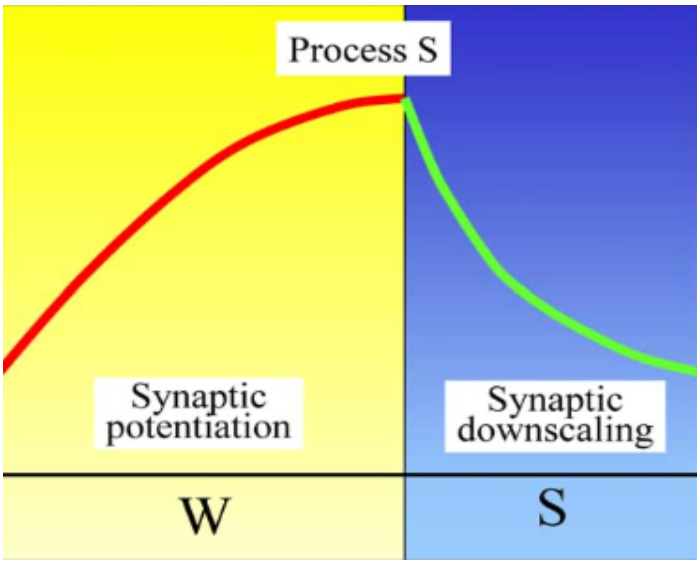

Figure 3: Overlay of synaptic homeostasis hypothesis theory on Borbely's Process S. *(Tononi et al, 2006 Figure 1.)*

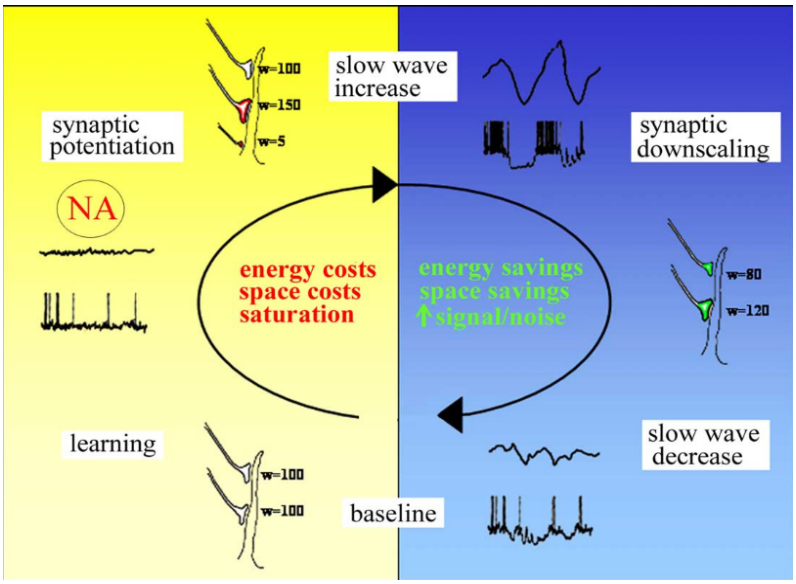

Figure 4: Diagram of the synaptic strength hypothesis. *(wake = yellow, sleep = blue). (Tononi et al, 2006 Figure 2.)*

EEG Correlates of Sleep and Wake

Sleep deprivation is an important tool used in the sleep field to understand how sleep is homeostatically regulated. By challenging the sleep homeostat through prolonged wakefulness, one can begin to tease apart its components and see how influencing various factors can affect subsequent sleep. Readouts of sleep regulation include EEG and neuronal activity. As outlined in Borbely's two process model, delta power is increased over time during wake and decreases during subsequent recovery sleep. Because of this observation, it considered a classical indirect measure of sleep pressure. Another indirect measure of sleep pressure is theta (5-9Hz). Power in this range has been shown to increase with time spent awake and decrease proportionally during sleep (Hung et al., 2013, Vyazoskiy et al., 2011). Recordings in humans have demonstrated that increases in theta during wake and SWA during NREM sleep occur appear the largest in the anterior portion of the cerebral cortex (Finelli et al., 2000). This finding suggests that the two EEG components may reflect similar processes (Hung et al., 2013).

While theta and delta are markers of sleep pressure, gamma frequencies (>30Hz) are associated with arousal. Gamma is highest during wakefulness, is intermediate in REM sleep, and is lowest during slow-wave sleep (Gross and Gotman, 1999). Gamma is also associated with sensory processing, focused attention and cognition and memory, as studies in humans and other mammals have shown that gamma frequencies increase during cognitive tasks (Gross and Gotman, 1999; Cardin, 2016).

Increasing evidence suggests waking experience can modulate the activity and architecture of subsequent sleep. A study in humans examined whether experience-dependent synaptic plasticity during sleep deprivation could result in differential wake

theta activity (Hung et al., 2013). This was done by having participants engage in 2 different tasks - listening to audiobooks or learning a visuomotor task. Both activities resulted in a global increase in theta activity. Regional task-dependent changes in theta were also seen and were found to correlate with local changes in NREM during subsequent sleep. The influence of different wake experiences has also been tested in mice. Activation of different brain regions during wake resulted in local increases in SWA, indicating that sleep is regulated in an activity-dependent manner at a local level (Vyazovskiy et al., 2011; Krueger et al., 2019; Milinski et al., 2021). A recent study in mice demonstrated that wakefulness dominated by wheel-running led mice to stay awake for longer than mice allowed to explore novel objects (Milinski et al., 2021). Despite these changes in wake, subsequent SWA was the same for both conditions. In contrast, mice allowed to performed a self-motivated operant task had increased SWA compared to those given novel objects. These results provide evidence of waking experience's influence on not only ensuing sleep but also the wakefulness period itself

Circadian Rhythms

Just as prior wake time and experiences can modulate sleep and wake state regulation, circadian rhythms also play an important role. Circadian rhythms were developed over the course of evolutionary time in response to changes in the Earth's axis and rotation around the sun. As a result, biological rhythms in behavior, gene expression and metabolism (among others) developed, providing organisms the ability to predict changes in various environmental variables including light levels, temperature and food availability. This predictive power provided an advantage over others who were unable to

do so and ultimately enabled the conservation of energy by upregulating certain behaviors and biological processes when they would likely be needed most (Deboer, 2018). Circadian rhythms occur over a period of approximately 24 hours and control things from arousal, alertness, body temperature, and food-seeking behavior. Externally, these cyclical patterns are entrained by cues including light, food intake and social interactions.

The internal timekeeper, or master pacemaker, of circadian rhythms is the suprachiasmatic nucleus (SCN). Located in the anterior hypothalamus, the SCN is important in the establishment and maintenance of these rhythms. In the absence of external cues, lesions of this region result in the inability to establish circadian rhythms (Eastman et al., 1984). This effect, however, can be reversed in the presence of some external cue. The SCN consists of approximately 10,000 neurons that work together to maintain synchronicity of various clocks within the body (Deboer, 2018). These molecular clocks, including the pacemaker itself, rely on the expression of clock genes, so called because they regulate circadian timekeeping. Two major players in this system are the genes *clock* and *bmal1*. The Clock and Bmal1 proteins form a heterodimer in the nucleus and activate the transcription of three *Period* (*Per 1-3*) and two *Cryptochrome* (*Cry 1,2*) genes. Cry 1 and 2 then participate in a negative feedback loop which reduces the transcriptional activity of Clock and Bmal1. Other genes such as *Rev-erb alpha, Rev-erb beta, Ror alpha* and *Ror beta* are also activated by the Clock/Bmal1 dimer and serve as modulators of Bmal1. Vasopressin, under the control of Clock, also participates in a similar feedback loop (Challet et al., 2007). Together, these genes underlie circadian rhythmicity and display differential expression patterns over time.

The contribution of circadian rhythms to sleep regulation has been studied using genetic knockouts for various clock genes in mice and flies. *Cry1* and *Cry2* double knockout mice exhibit behavioral arrhythmicity under dark-dark conditions in addition to increased NREM sleep and greater sleep consolidation (Deboer, 2018; Wisor et al., 2002). *Per1* and *2* double knockouts also display a similar increase in NREM sleep (Shiromani et al., 2004). Knockouts of various clock genes lead to different effects on sleep. In contrast to *Cry1, 2* mutants, mice lacking the *clock* gene display less sleep than wildtype animals despite their lack of locomotor arrhythmicity (Naylor et al., 2000). Evidence in *Drosophila* also points to the role of clock genes in sleep regulation. Loss of function clock gene mutant such as period (per^{01}) and clock (clk^{jrk}) displayed increased sleep rebound following 3, 6, 9, and 12 hours of sleep deprivation, eventually regaining all sleep time lost (Shaw et al., 2002).

Interestingly, the SCN itself does not have many direct connections to sleep-wake centers in the brain. Instead, it appears to regulate circadian rhythmicity of sleep via connections to the subparaventricular zone (SPZ) and the dorsomedial hypothalamic nucleus (DMH) which, in turn, project to sleep-wake populations. The densest connections from the SCN are to the SPZ. Lesions to this area, similar to those in the SCN, result in the inability to establish circadian rhythms. Rhythms affected include feeding, body temperature and sleep-wake cycles (Lu et al., 2001; Fuller et al., 2006). The ventral portion of the SPZ then projects to the DMH. Lesions in this area also prevent circadian rhythm development, particularly in locomotor activity, sleep-wake, feeding and some hormone secretion (Chou et al., 2003; Fuller et al., 2006).

Sleep-Wake Circuitry

Most insights about the regulation of sleep and wake were gained during the 20th century. The first hypothesis about how they are regulated was proposed by Baron Constantin von Economo in the 1920s, who noticed that people who fell sick with encephalitis lethargica exhibited increased sleep. Post-mortem examination revealed lesions in particular parts of the brain, providing a link between specific brain regions and the control of wake and sleep. Following von Economo's initial observations, many studies have demonstrated that sleep and wake states are promoted by a complex network of brain regions (Figures 5-7). Many of which are active during more than one sleep/wake state or respond to multiple external or interoceptive stimuli.

Wake promoting pathways ascend through the paramedial region of the midbrain and subsequently split into dorsal and ventral pathways. The dorsal pathway makes connections in the thalamus, while the ventral pathway projects to the hypothalamus, basal forebrain (BF) and cortex. For normal wakefulness to occur, both pathways must be intact. Inhibition of the dorsal pathway was shown to completely stop locomotor activity. Once lifted, locomotor activity resumes with little effects on wake time (Scammel et al., 2018). Injury to the ventral pathway results in increased difficulty staying awake and higher amounts of sleep (Fuller et al., 2011; Ranson, 1939).

Part of the ventral pathway, the BF contains three major sets of neurons: cholinergic, GABAergic and glutamatergic. This region is thought to be critical for promoting wakefulness and contributes to the high EEG frequencies which are characteristic of it (Saper and Fuller, 2017). The BF is well known for its large cholinergic neuron population, which exhibits high firing activity during wake and REM

sleep. Less activity is seen during NREM sleep. Lesions to this area cause permanent high voltage, slow state EEG activity associated with a lack of behavioral responsiveness. Further, optogenetic activation of all cell types in this region strongly promotes wake, providing more evidence of the important role of this area in wakefulness.

The BF receives inputs from the parabrachial (PB), pedunculopontine (PPN) and supramammillary nuclei. Glutamatergic neurons in the PB and PPN display firing activity patterns similar to the BF and also result in the cessation of behavioral wake and high EEG frequencies (Saper and Fuller, 2017). All cholinergic and some glutamatergic and GABAergic neurons in the PPN are most active during wake and/or REM sleep (Boucetta et al., 2014). The PB is thought to be critical for wake as it heavily innervates the BF and lesions to medial neurons or deletion of vesicular glutamate transporter (Vglut2) reduce wake and increase NREM delta power (Saper and Fuller, 2017). Interestingly, the PB receives inputs from areas which process information about various states including pain, nausea and hypercarbia, suggesting that it can promote arousal in response to a variety of stimuli. The supramammilary nucleus projects to the BF, cortex and to the hippocampus. While cortical connections from this nucleus strongly promote NREM sleep, hippocampal connections play a role in REM sleep.

Neurons that release monoaminergic neurotransmitters such as norepinephrine (NE), serotonin (5HT), dopamine (DA) or histamine are typically associated with arousal. These neurons innervate several regions including the cortex, BF, lateral hypothalamus, and thalamus among others (Scammel et al., 2018). The locus coeruleus (LC) is a large source of norepinephrine in the forebrain. It receives inputs from a variety of sources and is particularly active during high levels of arousal following strong stimuli such as stress,

reward or potential threats. The dorsal and median raphe nuclei are major sources of serotonin in the brain and receive inputs from various wake- and sleep-promoting areas (Calizo et al., 2011; Scammel et al., 2018). While the dorsal raphe is thought to play a role in wake, the median raphe has been shown to play a role in NREM sleep (Arpa et al., 1988). The ventral tegmental area (VTA) contains primarily dopaminergic neurons which are thought to be wake-promoting. Activation of these neurons or their connections in the amygdala and nucleus accumbens promotes wake, suggesting that this area promotes arousal in the context of high motivation (Scammel et al., 2018). The tuberomammillary nucleus (TMN) contains the only histaminergic cells in the brain and is known to activate regions associated with wake, including the thalamus and cortex. Because histamine levels are relatively high during arousal and application of histamine antagonists are sedating, histamine is thought to promote generalized wake. Some studies suggest that the co-release of GABA is important for wakefulness; however, this has not been definitively demonstrated (Scammel et al., 2018).

The lateral hypothalamus contains both wake- and sleep-active neurons. Wake-promoting neurons express orexin (hypocretin) and glutamate. They fire most rapidly during wake and their activation strongly promotes it (Saper and Fuller, 2017). Knocking out orexin causes narcolepsy by reducing the consolidation of wake and sleep states, further implicating the LHA's role in arousal. The LHA is thought to promote wakefulness in part due to projections to the reticular formation in the thalamus. Sleep-active neurons in this region primarily express melanin-concentrating hormone (MCH) and Vglut2. They are mostly active during REM sleep, but may also play a role in NREM sleep. These neurons differentially regulate other regions by releasing either glutamate or

GABA. It is unclear, however, which neurotransmitter expressed in the LHA promotes REM sleep (Saper and Fuller, 2017).

Major sleep-promoting regions in the brain include the ventral lateral preoptic area (VLPO), median preoptic area (MnPO), parafacial zone (PFZ), subcoeruleus region and ventral lateral periaqueductal gray (vlPAG). GABAergic cells in the VLPO and MnPO have been implicated in the generation of sleep. Lesions of VLPO neurons have been found to reduce sleep by 40% and their activation found to greatly increase it. While these preoptic nuclei are largely GABAergic, cells in the VLPO express the neuropeptide galanin. It is not known which neurotransmitter is responsible for their sleep-promoting activity. GABAergic cells in the PFZ are also active during sleep and are thought to promote this state by inhibiting the PB.

REM sleep is thought to be partly under the control of the subcoeruleus region. It contributes to muscle atonia by indirectly inhibiting motor neurons in the spinal cord and medulla and causes EEG desynchronization, although the mechanism behind this is not understood (Saper and Fuller, 2017). Nearby nuclei, including the PB, PPN, and laterodorsal tegmental area, also contain REM active neurons. Therefore, it is possible that an interaction between these regions is necessary for REM sleep generation. The vlPAG also regulates REM sleep, decreasing its amount via inhibitory projections to the subcoeruleus region.

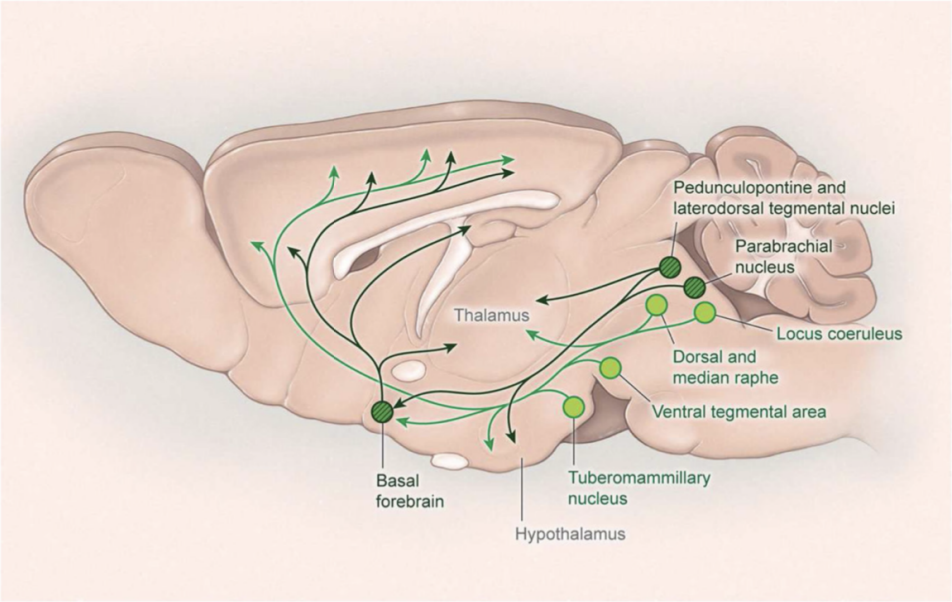

Figure 5: Wake-promoting brain regions
(Scammel et al., 2018)

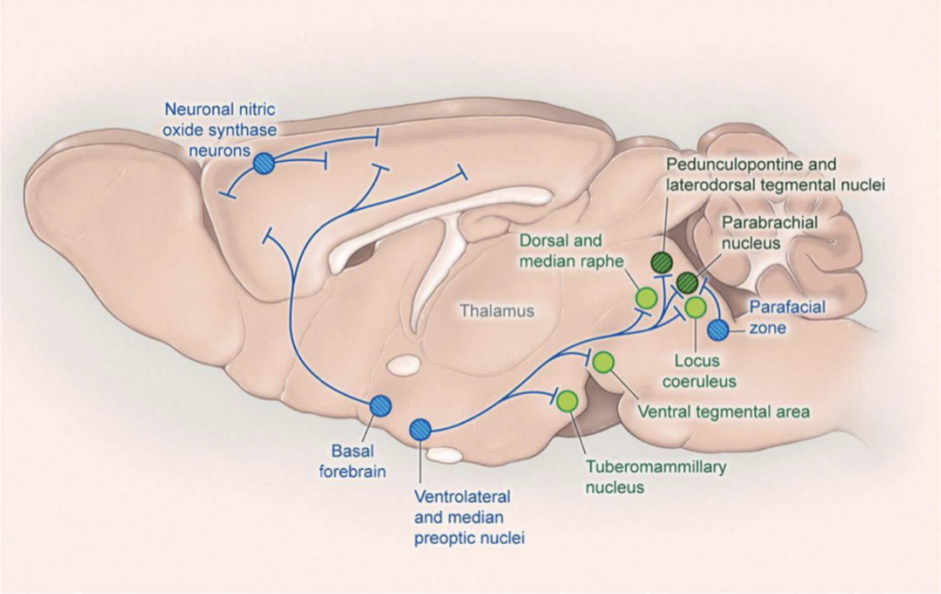

Figure 6: NREM-promoting areas.
(Scammel et al., 2018)

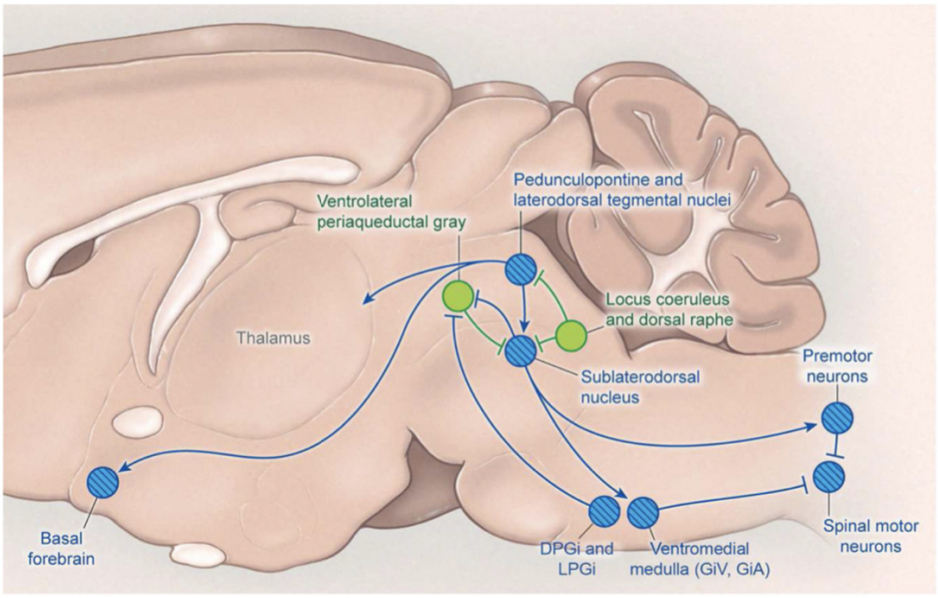

Figure 7: REM-promoting areas
(Scammel et al., 2018)

Chapter II.

Methods

Experimental Animals

Two strains of mice were used in this study: C57BL/6J (n=9) (B6) and Nms-iCre;Bmal1 (n=12). Nms-iCre;Bmal (Nms) mice were used to investigate the circadian component of sleep regulation and were generated by crossing the B6.129S4(Cg)-Arntltm1Weit/J (Bmal1) line, which contains two loxP sites surrounding the clock gene Bmal1, with the C57BL/6-Tg(Nms-icre)20Ywa/J (Nms-iCre) line. Nms-iCre mice express a codon-optimized Cre-recombinase in a subset of neurons in the suprachiasmatic nucleus that express neuromedin S. In the presence of Cre-recombinase, the exon containing the loxP sites and *Bmal1* gene are deleted. Deletion of *Bmal1* results in a loss of circadian activity in dark-dark conditions (24h lights off) (Lee et al., 2015). C57BL/6J mice were used as rhythmic controls. Male mice (12-24 weeks) were singly housed in customized cages (25cm x 25cm x 25cm) with food and water given *ad libitum*. Room temperature and humidity were maintained at 22°C ± 2°C and 40-70%, respectively. All experiments were approved by and conducted in accordance with regulations on animal experimentation set forth by the Veterinary Office of Basel City and the Animal Welfare Office of the University of Basel.

Surgeries

To measure brain activity during sleep and wake, experimental mice were implanted with an EEG implant. Thirty minutes prior to surgery, the animal received an

injection of the analgesics carprofen (5mg/ kg) and buprenorphine (0.1 mg/kg). During the procedure, isoflurane was used as an anesthetic and the level of anesthesia monitored via pedal withdrawal reflex and respiration frequency and depth. The implant was placed on top of the skull, with the two EEG screws placed above the cortex, just before lambda and bregma, and secured with dental acrylic. Following surgery, the mouse was returned to its cage to recover. A heating pad was used to provide thermal support during the procedure and subsequent recovery. Buprenorphine was injected again 4 hours after surgery. Subcutaneous injections of carprofen and/or buprenorphine were given for at least 2 days post-operatively. Additional doses were given on an as-needed basis.

Experimental Setup

Once fully recovered from surgery (approximately 7 days), mice were placed into a behavior rig, allowing for the single housing of one animal in each and monitoring via an infrared camera set up above the cage. To obtain EEG data while enabling free movement, each mouse was hooked up to a commutator and electrophysiological amplifier. Once placed in the rig, mice were allowed to acclimatize to their new environment for at least 1 week. Actual acclimatization time varied depending on the experimental group. C57BL/6J (rhythmic) mice were placed in a 12h light/dark (LD) cycle with lights on at 9:00. Following an initial acclimatization period in light/dark, Nms (arrhythmic) mice were placed in a 24-hour dark (DD) cycle for at least 4 weeks to eliminate circadian rhythms. Animals' movements were tracked using a video tracking program developed by the lab. Rhythmicity was monitored by plotting activity over time. During this period, baseline behavioral data was collected including EEG data and

locomotor activity. Experiments with arrhythmic mice occurred once loss of circadian rhythms was confirmed by looking at each animal's actigraphy.

Sleep Deprivation

Four sleep deprivation methods were utilized during this study, with each designed to engage mice in different behaviors. All behavioral experiments were performed during the subjective day. B6 and Nms mice were sleep deprived once per deprivation method for 5h, from 9:00 (ZT0) to 14:00 (ZT5) and were subsequently allowed to recover for 5h. A minimum of 3 days were kept between sleep deprivations to allow the mice to recover fully and to avoid any potential spilling over of effects from one deprivation to the next. Sleep attempts were defined behaviorally as the lack of locomotor activity and closing of the eyes. Behavioral sleep was confirmed as a sleep attempt by the EEG signal transitioning from a fast frequency, low amplitude signal to slow frequencies with a high amplitude. All deprivation methods used were developed to minimize the animals' stress during the deprivation period by limiting experimenter contact with the mice when possible and avoiding the use of noxious stimuli. Stimulus presentation was scheduled at 15-minute intervals to reduce variability in animal treatment. This scheme was followed unless a sleep attempt was made. A log was kept detailing the time of each sleep attempt and any associated notes.

Misting

Mice were sprayed with a fine mist of water using a spray bottle once at the beginning of the deprivation and then once every 15 minutes afterwards. In the event of a

sleep attempt, mice were quickly given one spritz to disrupt their entry into sleep. If a mouse made another sleep attempt within a few minutes, their nesting material was removed. When possible, at least 5 minutes was maintained between mists and the schedule followed. If taken out, nesting material was placed back in the mouse's cage following the 5h deprivation and mice were allowed to recover.

Novel Objects

Mice are curious in nature and readily engage in exploratory behavior when presented with unfamiliar objects. This kind of spontaneous exploration has been previously shown to be effective in promoting wakefulness and to result in corticosterone levels indistinguishable from control animals (Colavito et al., 2013; Hairston et al., 2005). In this paradigm, novel objects were placed in the cage of each mouse at 15-minute intervals or when the animal made a sleep attempt. Mice were not exposed to these items in advance. The order of the novel objects was kept consistent between experiments. Objects were chosen primarily based on their size, texture and shape, in addition to their experimentally observed ability to elicit different exploratory behavior in experimental animals. If an animal fell asleep before the scheduled object presentation, its nestlet material was first taken out. After this, a separate group of "extra" objects were used.

Objects used in this protocol were as follows (in order):

- Cryomold
- Styrofoam block

- Petri dish
- Nitrile glove
- Cardboard prism
- Bottom half of small pipette tip box
- Paper towel ball wrapped with lab tape
- Aluminum foil square
- 15mL seesaw (15mL Falcon tube taped to a cardboard rectangle)
- Open Easter egg
- Square of cardboard
- 50mL Falcon tube
- Sheet of paper (10cm x 28cm)
- Yellow foam square
- PCR tube strip wrapped in tape around base
- 50mL seesaw (same as 15mL, but using 50mL Falcon tube)
- Weigh boat
- Quarter of a PCR plate
- Plastic transfer pipette
- Kimwipe

Extra objects used (in order):

- Partial face mask
- Crumpled piece of paper (10cm x 28cm)
- 50mL Falcon tube top with strips of paper attached

- 15mL Falcon tube

Burrowing

This protocol was designed to elicit engagement in the form of natural digging, or burrowing, behavior in mice. Square plastic bottles were designed with a slit at the top, along the length of the bottle, so as to permit entry of an EEG-implanted mouse. Bottles were filled completely with food pellets and one placed in the corner of each cage at the beginning of the deprivation. Mice were pre-exposed to the bottle for a three-day period before the experiment to familiarize them with it and to encourage digging during the deprivation. Mice who failed to remove any pellets were excluded. On the day of the experiment, a bottle was placed in the cage and any pellets removed by the mouse after 15 minutes were placed back in the bottle. A second, new bottle then replaced the first. Bottles were weighed before and after being placed in the cage to keep track of the amount of pellets moved. Two were alternated every 15 minutes. In the event of a sleep attempt, a new bottle was placed in the cage before the scheduled presentation. Care was taken to keep bottles from one cage together so as to avoid presenting one mouse with the scent of another.

Flouring

The same procedure followed for misting was used in this paradigm. Instead of being misted with water, however, mice were presented with a "puff" of flour. A plastic transfer pipette was used to provide the stimulus once every 15 minutes or when an

animal fell asleep. Each time, a small amount of powder was picked up by the pipette and one “puff” administered.

EEG Signal Processing and Analysis

EEG data was collected using the Spike2 software (Cambridge Electronic Design Limited, Cambridge, England). Data was preprocessed using a customized pipeline which clusters and classifies sleep and wake states using deep neural networks, linear discriminant analysis and density peak clustering. Based on density peak clustering, wake was classified into two substates: high theta and low theta wake (HWake and LWake, respectively). In some animals, the boundary between HWake and LWake was difficult to define using the density peak clustering algorithm. In these cases, both states were annotated as ‘Wake’ and data from these animals was excluded from further wake analysis. It is unclear why this occurred in some mice and not others. It is unlikely, however, that this is due to EEG placement, as EEG placement was standardized across mice.

Data Extraction and Statistical Analysis

EEG data was extracted using custom PyCharm scripts. Statistical analysis was performed in GraphPad Prism. Two-way ANOVAs were used to determine the effect of various deprivation methods during sleep deprivation (SD) and recovery sleep (RS) in each sleep and wake state and between arrhythmic and rhythmic mice. A 95% confidence interval for the data on cumulative amounts of recovery sleep was found using PyCharm.

2D section pipeline

Tissue Collection

B6 mice (n=9) were sleep deprived using the Misting protocol and were euthanized via isoflurane overdose 1, 3, and 5 hours into sleep deprivation (SD1, SD3, and SD5, 3 per timepoint) to see how brain activity changes over time during prolonged wakefulness. Mice were perfused with phosphate-buffered saline followed by 4% paraformaldehyde (PFA). Brain tissue was collected and stored at 4°C overnight in 4% PFA and then switched to 30% sucrose solution for two days. Samples were then moved to a cryomold and submerged in O.C.T compound for storage at -80°C.

Histology and Imaging

Coronal sections 50μm thick were cut via a cryostat starting from the end of the olfactory bulb until the end of the cerebellum. All sections were collected for immunohistochemistry. Tissue was stained using an anti-c-Fos primary antibody (1:2000, rabbit, Synaptic Systems, 226 003) and stained with anti-rabbit Alexa 647 (1:1000, Thermo, A32795). Sections were then mounted on SuperFrost Plus slides (60cm x 20cm) from Thermo Scientific using a Fluoromount-G Mounting Medium with DAPI. Slides were imaged using the ZEISS AxioscanZ.1 Slide Scanner.

Virtual Alignment of Sections

Prior to cell quantification, all sections were aligned using the TrackEM2 ImageJ plugin to ensure all sections were in the correct order from posterior to anterior and were aligned with the previous section in the image stack. Left and right orientation was also kept consistent.

Manual Cell Detection

c-Fos+ cells were counted as described below using ImageJ. A particular region of interest within the brain was selected and its location identified within the sections by looking at both DAPI and Fos channels. Prior to quantification, the Fos channel images were merged with the approximate corresponding atlas image from the Allen Brain 2017 mouse reference atlas. The outline of the region was traced as an ROI to better define region boundaries based on both the atlas and the particular section being used. The images were then separated. A Gaussian blur filter was applied to the Fos channel and the image binarized. The watershed function was then applied to separate cells that were clumped together. The ROI selected from the atlas image was then copied to the Fos image and the number of cells detected were quantified using the Analyze Particles function. Circularity was set to 02.-1 and size to 12-200. This process was applied and cell counts recorded for every section containing the region of interest.

Warping of the Reference Atlas

The Allen Brain 2017 mouse reference atlas API was used to obtain annotated 32-bit images (10μm apart) of the adult mouse brain. Pixels in these images contain a unique value corresponding to a particular brain region as noted in the Allen API. This reference

atlas was opened in ImageJ using the BigDataViewer Plugin. Fos sample images were opened up as a stack alongside the Plugin window. Using the sample images as a reference, the Allen reference atlas was rotated from a coronal view about its Y and Z axes until the atlas was at an angle that matched the angle of the Fos sections. The appropriately rotated atlas was then exported as Tiff files.

Opening up the newly exported atlas images next to the Fos sections, the atlas image number which corresponded to each of the Fos sections was determined. Atlas images were warped to the Fos images using their DAPI channel as a reference. The ImageJ Landmark Correspondences plugin was used to select appropriate landmarks between the atlas and Fos images. In this way, the atlas was then warped to match the contour of the actual samples. This process was repeated for each Fos section. Each warped atlas section was renamed to the corresponding Fos image name and saved.

Automatic Cell Detection

A customized script for detecting Fos+ cells developed by the lab was used to identify active neurons (Figure 8). This script creates a histogram of intensity values within an image and subtracts background intensity levels while increasing the slope of peak values corresponding to Fos+ cells. The center of these peaks were calculated and a single pixel value outputted. Fos sample images were run through this script and centroids for each section were outputted as 8-bit Tiff files.

Warped atlas images and centroid files were then used to determine the regional location of each Fos+ cell in the Fos images. This was done via a custom-written Python script. Using the centroid file, a mask was created of coordinates corresponding to Fos+ signals. This mask was then applied to the warped atlas sections and the number of

unique pixel values was counted, representing the number of Fos+ cells per brain region. The count of unique pixel values in the atlas sections on their own was obtained to provide information about pixel size of each brain region. The density of Fos+ cells per brain region was quantified. Information regarding Fos+ cell count, region pixel size and density index for each section was calculated for each section and combined to provide information for whole brain regions (Figure 8). Whole brain activity information was then saved as a csv file for data analysis.

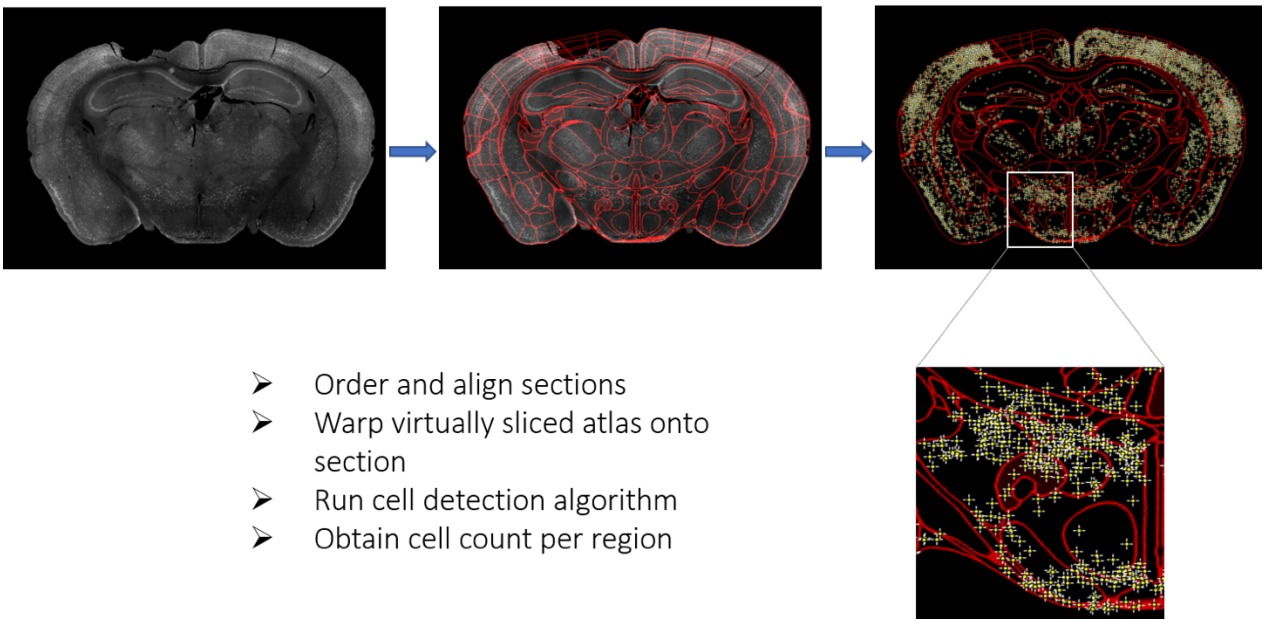

Figure 8: Schematic of automatic 2D section pipeline.

Chapter III.

Results

To begin to elucidate the homeostatic mechanisms underlying prolonged wakefulness and recovery sleep, four different sleep deprivation methods were used, each designed to take advantage of mice's innate reflexes and behaviors. The effects of each protocol on sleep-wake EEG activity and sleep architecture were compared among animals. These effects were then compared in mice with and without intact circadian rhythms to shed light on how the circadian clock effects the regulation of arousal and sleep states. As a complement to such studies, an image analysis pipeline was created for use in whole-brain reconstruction of sleep-wake circuitry using immediately early gene expression patterns.

This study is part of a larger, collaborative project with two postdoctoral fellows in the lab who are interested in sleep homeostatic regulation. These individuals performed the EEG implantation surgeries and assisted me with sleep deprivations. Classification of sleep and wake states and cell detection of Fos+ cells were made possible with their contributions. I performed all sleep deprivations and wrote custom Python scripts for data analysis and the creation of the 2D pipeline with help as described above. Histology of coronal sections and manual and automatic cell counts were done collaboratively.

Method Comparison

Wake behavior, sleep attempts and state transitions

C57BL/6J mice were sleep deprived at the beginning of the light period for 5 hours using one of four sleep deprivation methods: Burrowing (n=9), Misting (n=9), Novel Objects (n=9), and Flouring (n=4). Sleep deprivations occurred in four rounds, one per protocol, and were spaced 3 days apart to allow mice to fully recover in-between. Individual animals served as their own controls. Each protocol produced different behavior in the mice. Following a spritz with water during Misting, all animals were seen to engage in stereotypical grooming behavior in an attempt to remove water from their fur. While Misting was effective at preventing sleep attempts for an hour, mice began to nest and make sleep attempts during the next few hours. Toward the end of the deprivation, mice didn't engage as readily in grooming behavior, sometimes neglecting to do so after mists. Over time, it became increasingly difficult to keep the mice awake and multiple sleep attempts were seen. During the Novel Objects (NO) protocol, mice's behavior was less predictable. Mice engaged in a variety of behaviors including sniffing, chewing, climbing on and dragging objects. The amount of time each animal spent actively exploring and interacting with each object varied; however, mice consistently displayed much less nesting behavior or periods of inactivity than during Misting. Burrowing also resulted in less nesting and inactivity relative to Misting. Mice reliably removed pellets from each bottle presented to them over the course of the deprivation. The amount of time spent digging and the number of pellets moved varied with each mouse. Flouring was used as a kind of control for Misting, as it involved a similar stimulus administration scheme but lacked the "wet" component. Animals seemed largely

unbothered by the puffs of flour administered and exhibited little to no grooming behavior compared to Misting. After an hour, the mice were visibly tired and it became extremely difficult to keep them awake.

The number of sleep attempts made by the mice in each deprivation were recorded (Figure 9). A Two-Way ANOVA followed by Tukey's post hoc tests were performed. In the first hour of the deprivation, no sleep attempts were made. A steady increase in sleep attempts over time for Misting and Flouring can be observed, with the latter resulting in significantly more attempts to fall asleep relative to the other conditions. After two hours, mice exhibited sleep attempts in both Misting and Flouring. Flouring resulted in more attempts than all other deprivation methods, displaying the greatest increases over Novel Objects and Burrowing ($p<0.0001$). In hour 3, Flouring and Misting were higher than both NO and Burrowing. No significant differences between the former two were seen at this timepoint. After 4 hours, the number of sleep attempts in Flouring surpassed those in Misting and an increase in the number of sleep attempts during Burrowing can be seen. In the last hour of deprivation, mice fell asleep an average of 10.75 times in Flouring, 2.78 times in Misting, 2.22 times in Burrowing and 0.56 times in NO. Throughout the deprivation, NO displayed the smallest number of attempts over time, followed by Burrowing.

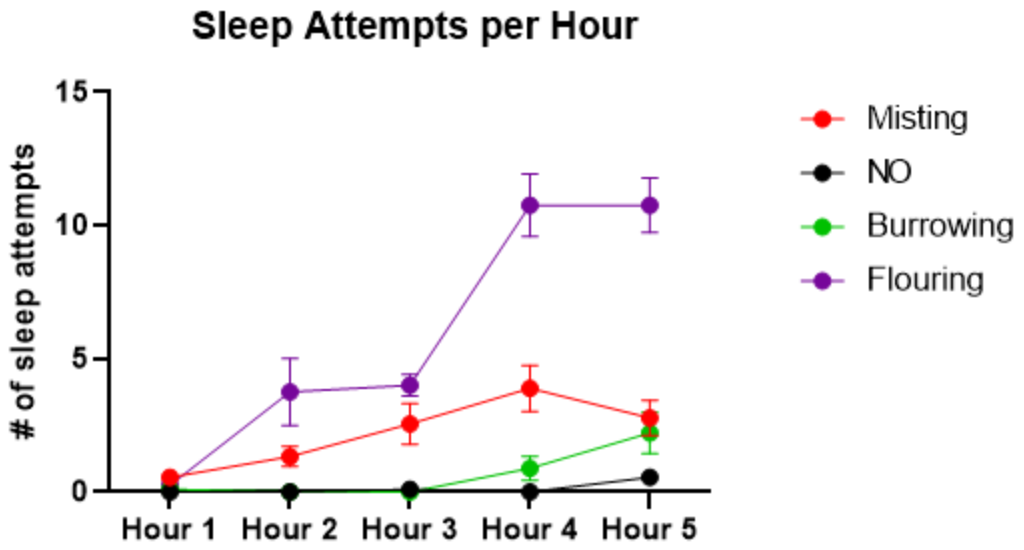

Figure 9: The number of sleep attempts over time per deprivation method.
Significant increases in Flouring and Misting can be seen throughout the 5h deprivation period relative to NO and Burrowing.

Given the differences in sleep attempts made during the deprivation period in each sleep deprivation protocol, it was hypothesized that the sleep and wake state distribution of the mice during the experiment would differ depending on the protocol used to keep them awake. Based on EEG data obtained, a deep neural network was used to classify data into 4 states. States were then projected onto a 3D subspace (see methods for more details). The states for one mouse are shown in Figure 10. The distribution of states the mouse was in during the first two (Early) and last two (Late) hours of each deprivation is plotted in red (Figure 10). Notably, Misting and Flouring display a high degree of transitions between Wake and SWS not seen in Burrowing or Novel Objects. This provides further evidence of the lower efficacy of these protocols in keeping mice awake. Interestingly, NO results in a higher concentration of points near the HWake cloud and fewer points low in the LWake cloud. Conclusions from this visualization of a

mouse's state space is supported by the data showing a significantly higher number of sleep attempts in Misting and Flouring over time (Figure 9).

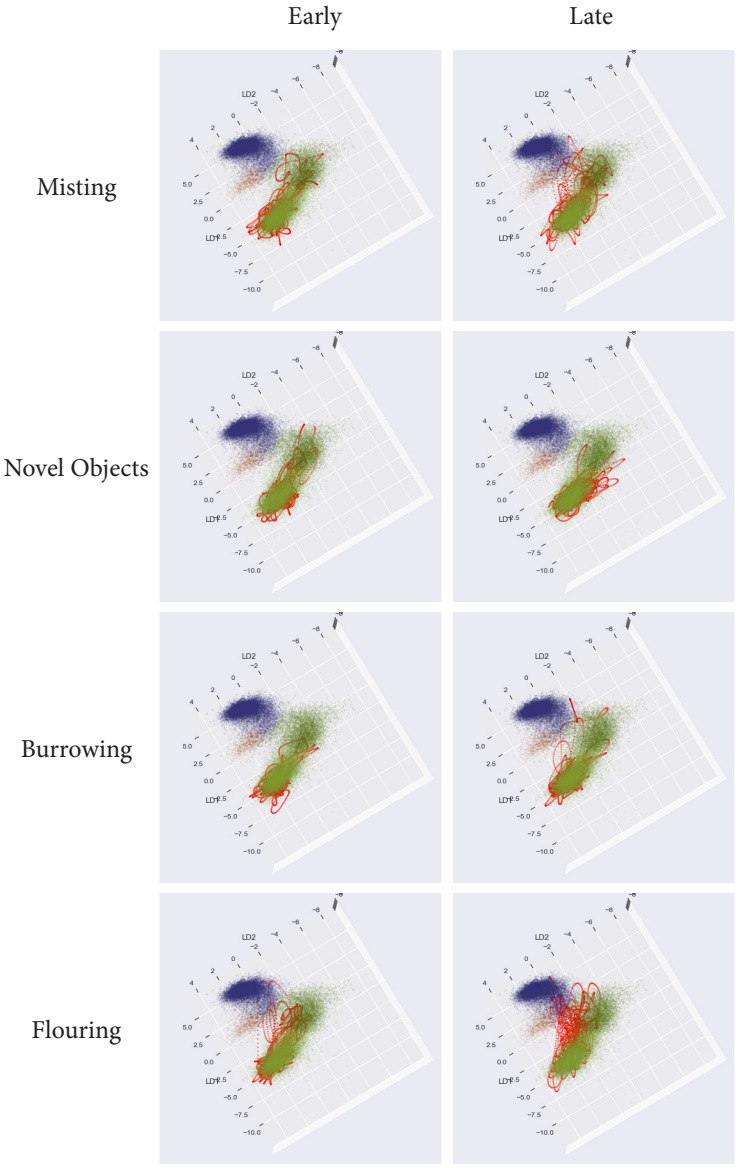

Figure 10: State space visualization of one mouse's state distribution during the first two (early) and last two hours (late) of each deprivation method.
Points correspond to datapoints obtained from the EEG recording and are color-coded based on the states to which they belong. (Color code: HWake - light green, LWake - dark green, SWS – purple, REM – orange.) Points in red are those the mouse was in during a given deprivation.

Power Spectral Analysis

Power spectral analysis has been a key tool used in the sleep field to understand state-specific patterns in brain activity (Achermann, 2009). This type of analysis has revealed that increased power in the delta and theta frequency bands correlate with increased sleep pressure (Borbely, 1982; Hung et al., 2013; Ehlen et al., 2013). To understand how brain activity changes over the course of sleep deprivation and recovery sleep and how these changes differ between deprivation protocols, the mean power per frequency bin was plotted for each state (Figure 11, 12). In this way, protocol-specific changes in spectral power could be more clearly seen. In HWake, a distinct misting-specific peak occurs in the range between 2-8Hz from early to late SD. To test whether this peak is due to the use of water as a stimulus in Misting, Flouring was introduced as an experimental method. Although much smaller than that in Misting, a peak in the same 2-8Hz region is also seen in Flouring (Figure 13). This suggests that the presence of the 2-8Hz peak seen in late SD for Misting is likely not due solely to water being used as stimulus but may be the result of the type of deprivation administered. A NO-specific signature also appears within this range, with the slope of line in these frequencies decreasing over time. Interestingly, both NO and Burrowing have higher power in the gamma (30-50Hz) range relative to Misting.

In LWake, all methods show increased power between 2-8Hz range from early to late. Misting and NO appear to have higher power in this band than NO in the early timepoint. This difference disappears, however, during late SD. Notably, NO exhibits a greater increase in power over time, with a change in peak height from approximately

9dB to 14.5 dB (Δ5.5dB) compared to a change from 12dB to 14dB (Δ 2dB) and from 12 to 15.5dB (Δ 3.5dB) for Misting and Burrowing, respectively (Fig. 11).

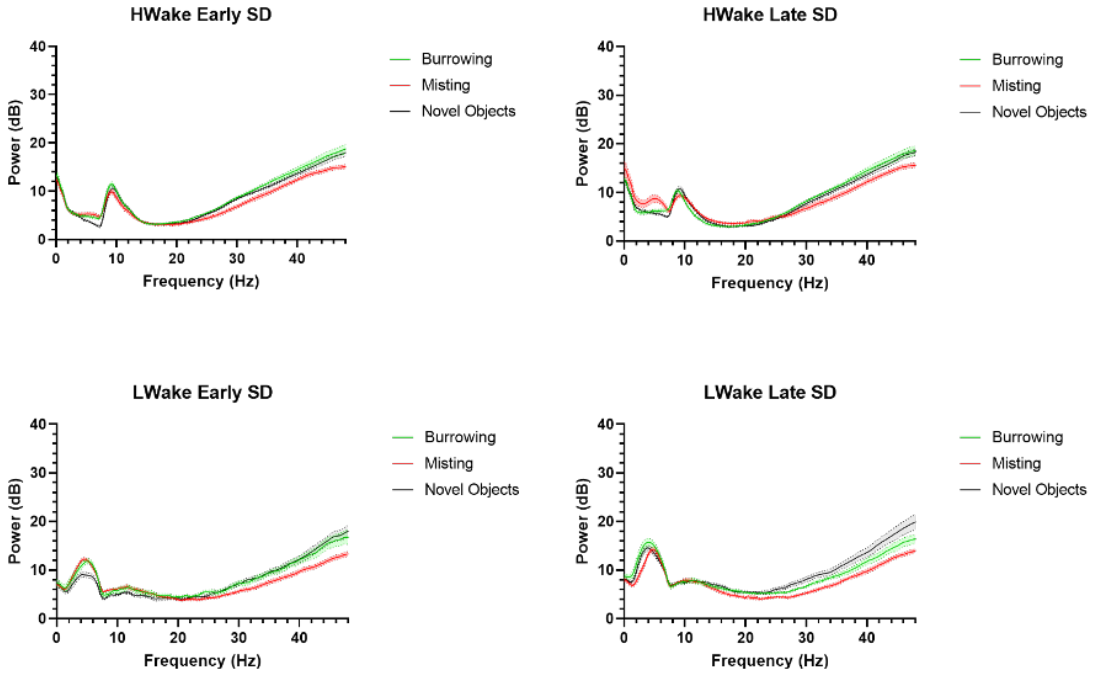

Figure 11: Average power per frequency bin between different protocols at early and late SD timepoints.
Upper: Comparison of HWake power over frequencies 0-50Hz for early and late SD between deprivation methods. Lower: Comparison of LWake power for early and late SD between methods.

Mice were allowed to recover for 5 hours following the SD period. All deprivation methods show a decrease in power during SWS from early to late RS in the 2-10Hz frequency band, consistent with the idea that delta and theta power decrease during sleep following prolonged wakefulness (Fig. 12). While clear trends can be seen

in other sleep and wake states, there were no noticeable differences in REM sleep over time between SD protocols.

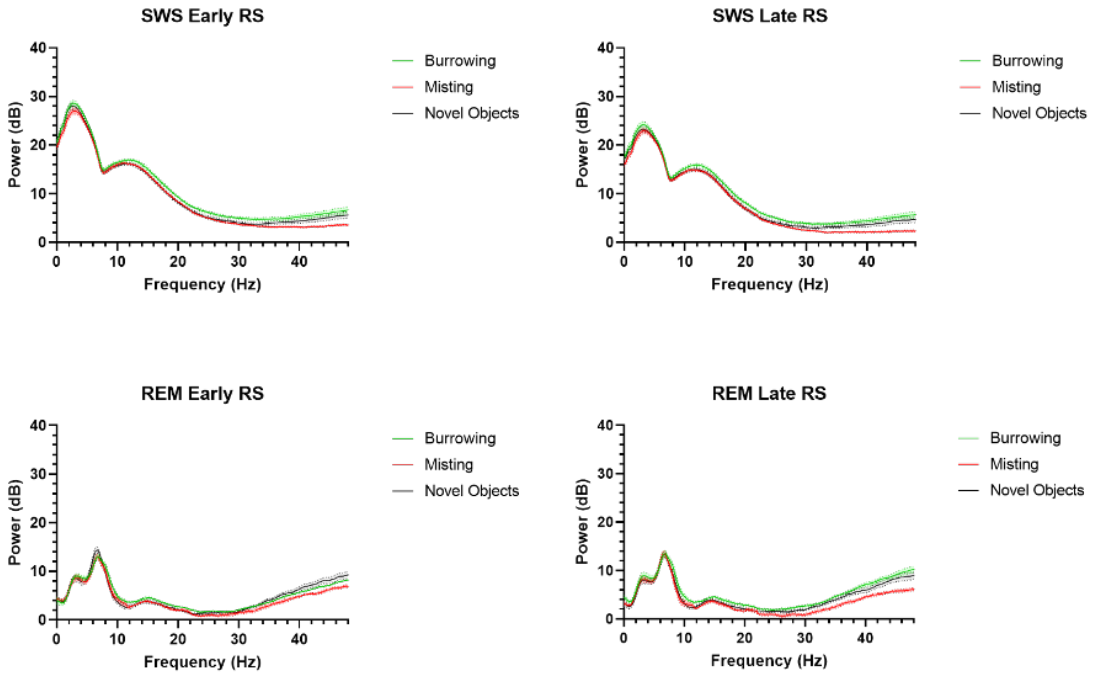

Figure 12: Average power per frequency bin compared between different protocols at early and late RS timepoints.
Upper: Comparison of HWake power over frequencies 0-50Hz for early and late RS between deprivation methods. Lower: Comparison of LWake power for early and late RS between methods.

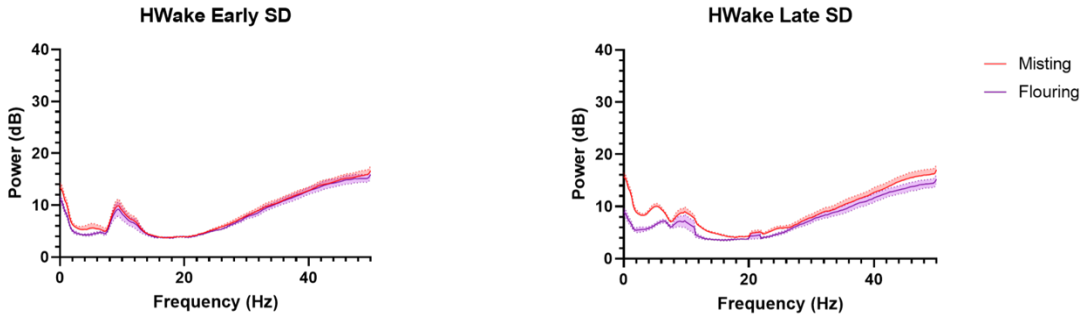

Figure 13: Comparison of HWake power spectrum in Misting and Flouring during early and late SD.

Because increases in delta and theta frequencies during SD and their subsequent decreases during recovery are used as hallmarks of rising and falling sleep pressure, respectively, the mean power of delta and theta were compared over time for each deprivation method (Figure 14) (Borbély, 1982, Hung et al., 2013, Vyazoskiy et al., 2011). Paired t tests were used to evaluate significance between early and late for each deprivation. Each band is defined differently depending on the study. Here, delta was defined as 1-4Hz and theta as 7-10Hz. A significant increase in delta between early and late was seen in Misting for HWake, while significant increases in theta were seen in both Misting ($p < 0.05$) and NO ($p < 0.0001$). Significant increases in delta and theta power over time occurred with all deprivation methods in LWake, with the highest differences seen in Burrowing and Novel Objects in the delta range and in Novel Objects in the theta range ($p < 0.001$) (Fig. 14). SWS exhibited the opposite trend of HWake and LWake, with significant decreases in both delta and theta from early RS to late RS ($p < 0.0001$).

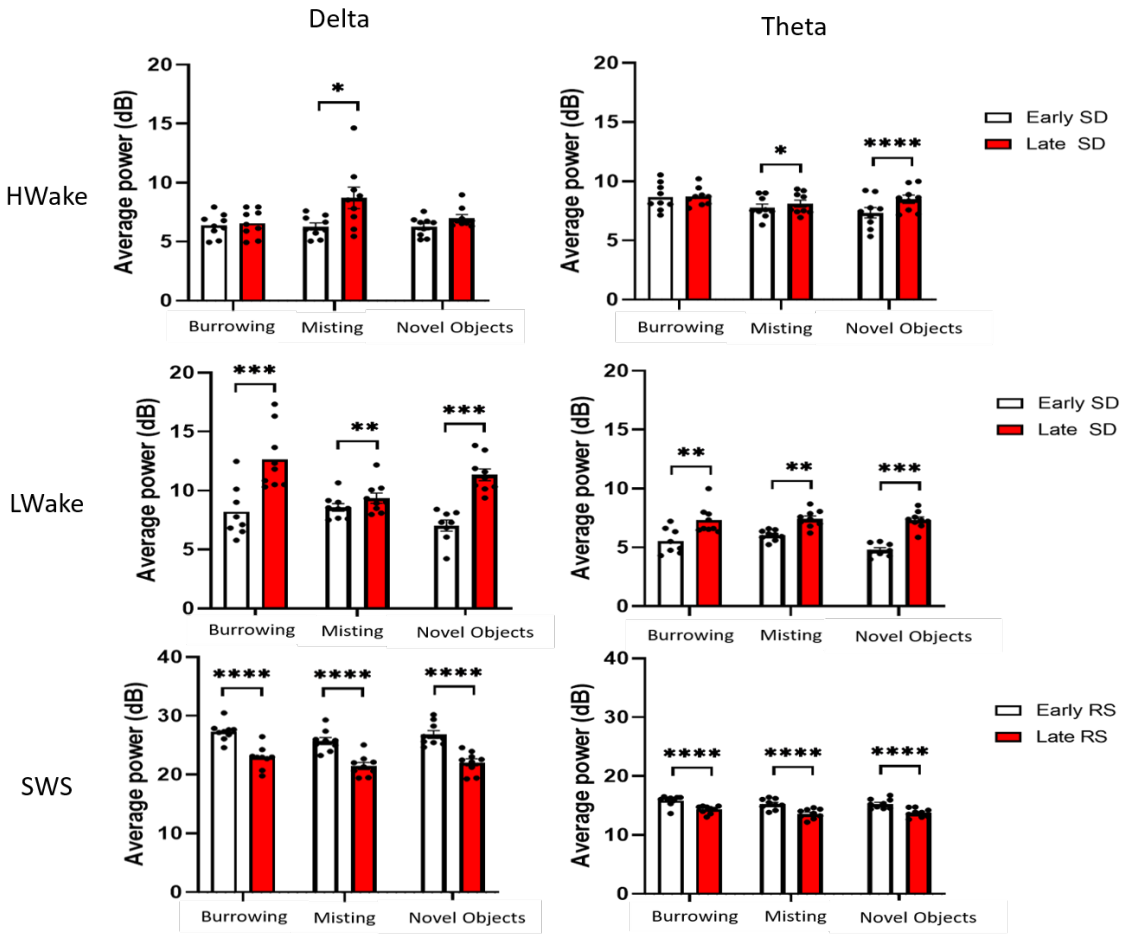

Figure 14: Average delta and theta power per state.
Comparison of delta (1-4Hz) and theta (7-10Hz) for Burrowing, Misting and Novel Objects. Early and late SD timepoints were compared for HWake and LWake and early and late RS for SWS.

Strain comparison

Baseline differences

To examine the effects of circadian rhythms on sleep and wake states during and after sleep deprivation, Nms mice were placed in DD conditions and were allowed to become arrhythmic. Once a loss of locomotor circadian rhythmicity was confirmed via actigraphy, arrhythmic mice were sleep deprived with Misting (n=8), Novel Objects (n=8) and Burrowing protocols (n=3). In the Nms group in particular, it was not always possible to computationally subclassify wake into HWake and LWake. Therefore, only data from Nms mice where these states could be separated were included in the wake analysis (Misting, n=8; NO, n =8; Burrowing, n=2). SWS and REM sleep were not affected. Prior to comparing the effects of each method on this group with rhythmic mice, baseline differences between the two groups were determined. Because Nms mice that have become arrhythmic do not have consolidated periods of wakefulness like the B6 mice, it was hypothesized that the percent of time spent in each state at baseline (no experimental manipulation) would be different between the two strains. Interestingly, Nms mice spend significantly less time in HWake ($p < 0.0001$) and more time in LWake ($p < 0.05$) (Figure 15). The percent of time spent in SWS was also increased in Nms animals relative to B6 mice ($p < 0.0001$). No significant difference was seen in REM sleep between groups.

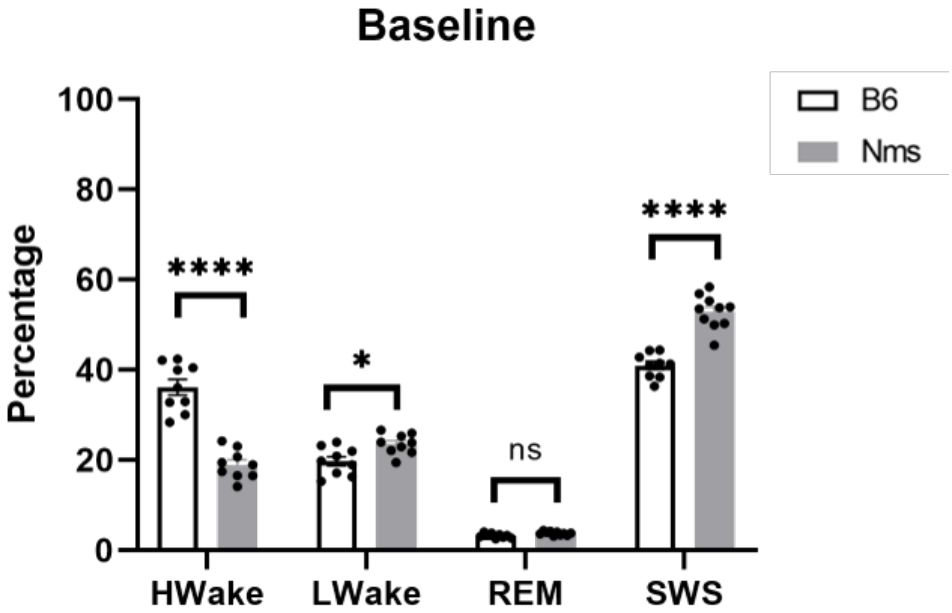

Figure 15: Percent of time in each state during baseline per strain.
Comparison of time spent in each state at baseline between rhythmic and arrhythmic mice.

Deprivation and Recovery

When looking at the deprivation or recovery sleep period as a whole, significant differences between the two strains were seen in Misting and Burrowing (Figure 16). After 5 hours of Misting, Nms mice spent a greater percentage of time during recovery sleep in LWake than B6 mice ($p < 0.01$). Rhythmic mice, however, spent more time in SWS ($p < 0.001$). No significant differences between strains were seen in Novel Objects. REM sleep was higher in rhythmic than arrhythmic mice during recovery following Burrowing ($p < 0.01$). Notably, no differences were found in the percent time spent in each state during the deprivation itself.

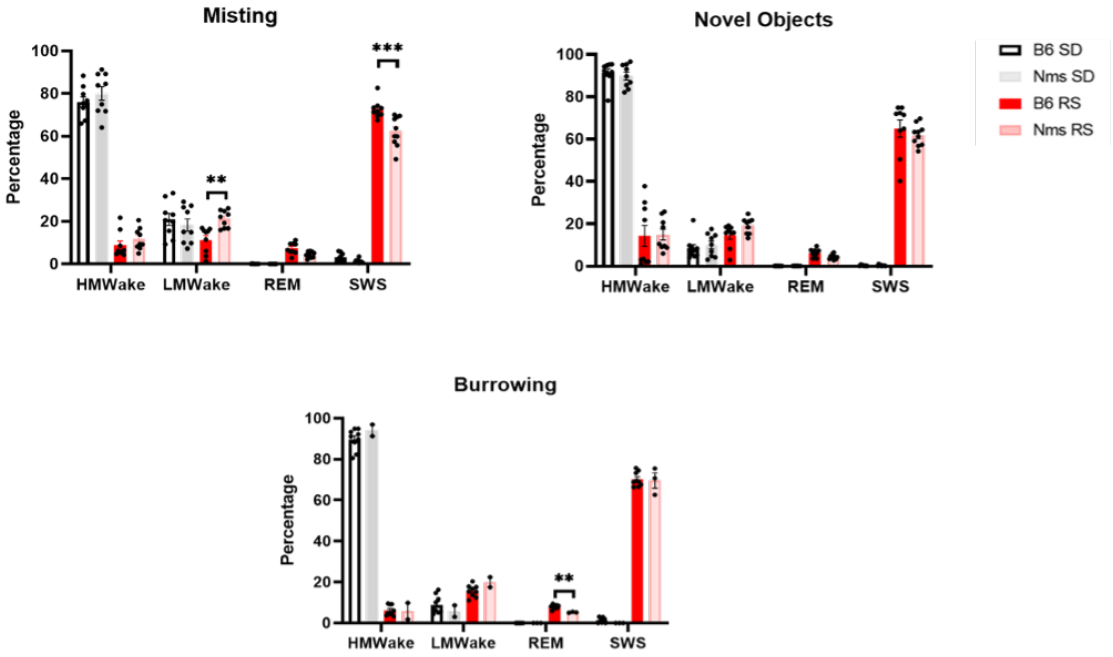

Figure 16: Percent of time in each state during SD and RS per strain.

Comparison of time spent in HWake, LWake, REM, and SWS for Misting, Novel Objects and Burrowing for early and late SD and RS.

Sleep Architecture

Studying sleep architecture provides insights into the quality of sleep and is important in understanding how disturbances in wake and sleep periods affect sleep homeostasis. The cumulative amount of time spent in SWS and REM during the 5-hour

recovery period following SD were quantified for both rhythmic and arrhythmic animals (Figure 17). Overall, B6 mice spent more time in SWS and REM than Nms mice across all deprivation methods. B6 spent an average of 210.2 ± 9.3 mins in SWS in Burrowing, 220.0 ± 9.5 mins in Misting and 214.6 ± 7.3 mins in NO (Fig. 17A). Nms mice, on the other hand, spent an average of 180.0 ± 7.2 mins of SWS in Burrowing, 185.7 ± 11.1 mins in Misting and 174.5 ± 16.3 mins in NO (Fig. 17B). This corresponds to Nms mice exhibiting 14%, 15.6%, and 18.7% less SWS than B6 mice in the first 5 hours following Burrowing, Misting and NO, respectively. Based on the cumulative plots, latency to fall asleep appears greatest for Burrowing in both rhythmic and arrhythmic animals. In both B6 and Nms mice, Misting results in the greatest amount of SWS over the 5 hour recovery period, followed by Burrowing. The least recovery SWS was seen in Novel Objects (Figure 17A, B).

B6 mice spent an average time in REM sleep of 22.8 ± 2.4 mins in Burrowing, 22.0 ± 3.9 mins in Misting and 22.5 ± 3.7 mins in NO (Fig. 17C). In contrast, arrhythmic mice spent an average of 13.2 ± 0.6 mins in Burrowing, 13.3 ± 3.1 mins in Misting and 12.4 ± 2.7 mins in NO (Fig. 17D). Nms exhibited nearly 50% less REM sleep than B6 in RS following Burrowing, Misting and NO (42%, 40% and 45% less, respectively). REM latency appears shortest after Misting for both rhythmic and arrhythmic animals, followed by NO and Burrowing. All deprivation methods in both strains have very

similar amounts of cumulative REM sleep, which may reflect the importance of the conservation of REM sleep (Fig. 17 C, D).

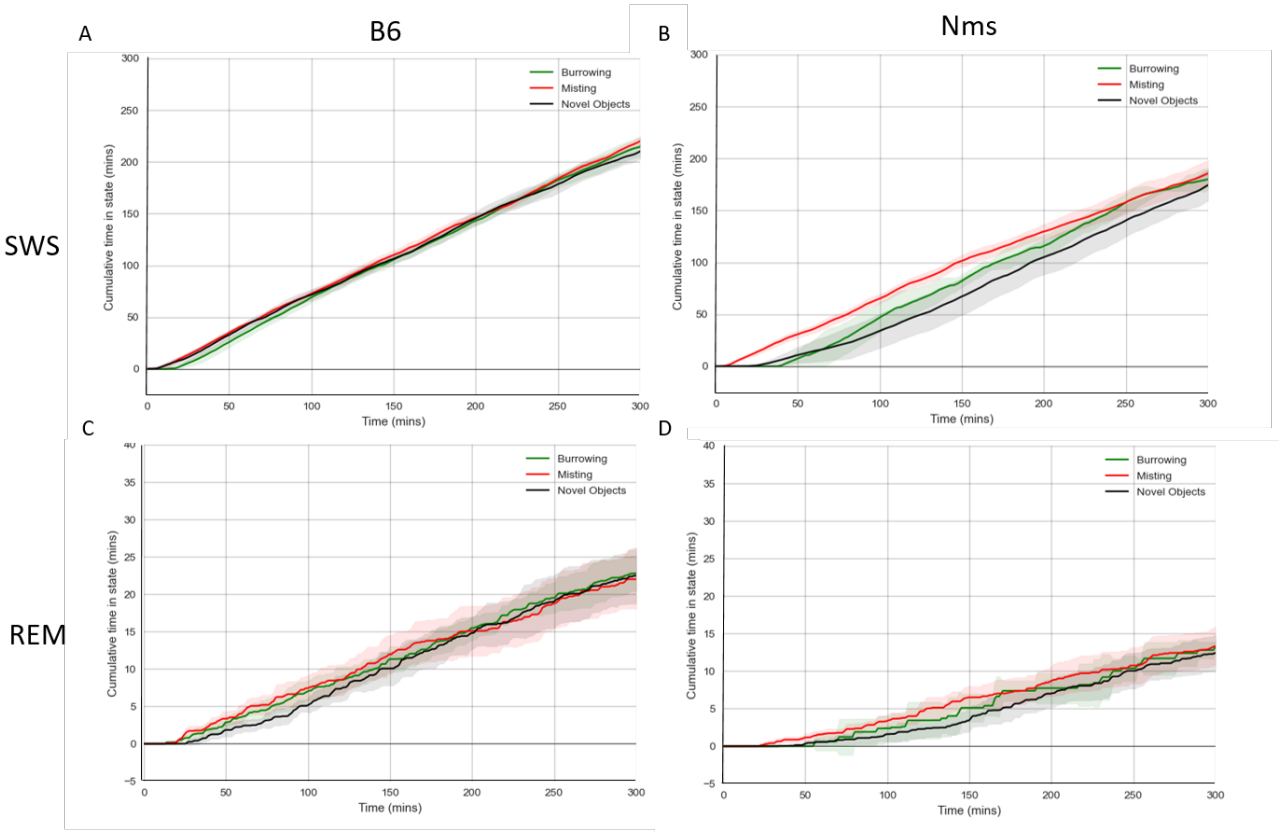

Figure 17: Cumulative time spent in SWS and REM during recovery following SD. *Upper: Comparison between deprivation methods of cumulative time spent in SWS for (A) B6 mice and (B) Nms mice. Lower: Comparison between deprivation methods of cumulative time spent in REM sleep for (C) B6 mice and (D) Nms mice.*

Pipeline outputs

Measures of Fos+ cells, pixel counts and density index for each brain region was run through a Python script allowing for data to be extracted regarding activity trends over time. One mouse was evaluated per timepoint (SD1, SD3 and SD5). For each brain region, a linear polynomial function was fitted to the data from SD1 and SD5. The coefficient, or slope of the line, was saved. The residual, or the difference between the values obtained in SD3 and those expected if the data were to follow the linear trend fit to the SD1 and SD5 datapoints, was calculated. The coefficient and the residual for each brain region were then plotted to display regional trends over time (Figure 18.) Each point corresponds to a given brain region. The script contains an interactive feature which allows the user to click on a given point and its regional identity to be displayed. Particular regions of interest can also be highlighted, as displayed in Figure 18. The points corresponding to the Central Superior Raphe (CS), Dorsal Raphe (DR), Barrel Cortex (SSp-bfd4), Lateral Hypothalamus (LHA) and the lateral division of the central nucleus of the amygdala (CEAl) are shown for demonstration purposes. A positive coefficient means that the data increases over time from SD1 to SD5, while a negative coefficient means activity decreases with time. A positive residual indicates that the SD3 timepoint has higher values than would be predicted for a linear increase over time. A negative residual means the value is lower than what would be expected. Looking at the Barrel Cortex, for example, this region increases rapidly over the course of SD and has a Fos+ cell count in SD3 that is higher than expected for a linear trend (Fig. 18).

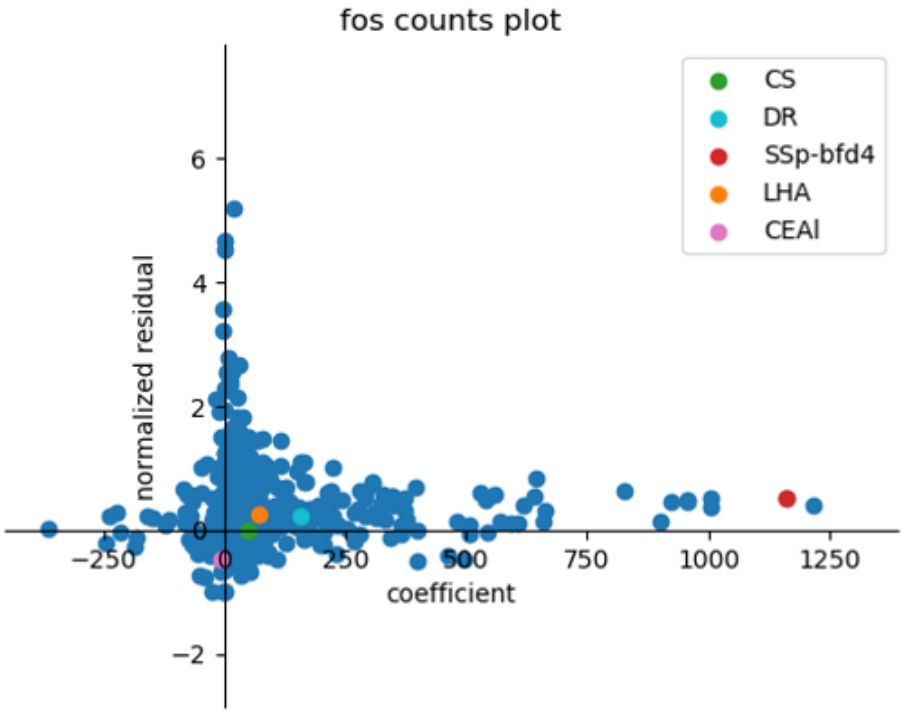

Figure 18: Regional activity trends over time.
Fos+ cell counts across all brain regions extracted using automatic 2D pipeline. The Central Superior Raphe (CS), Dorsal Raphe (DR),

Comparison of Automatic versus Manual Cell Counts

To verify that the Fos+ cell counts obtained per region using the 2D section pipeline were accurate, trends in automatically acquired data were compared to those in cell counts obtained manually. Cell counts and density indexes for two sleep-wake related regions were assessed (Figures 19, 20). The dots on the Fos+ cells and density index subplots in the automatically acquired data correspond to the values predicted at

each timepoint if a linear trend from SD1 to SD5 were followed. In the CS, trends in both the Fos+ cell counts and density index in the automatically acquired data indicate a very linear trend in activity over time from SD1 to SD5 (Fig. 19). Looking at the Density Index plot, one can see that the actual density index value at the SD3 timepoint is slightly higher than expected. These same trends can be seen in the data reflecting Fos+ cells counted by eye.

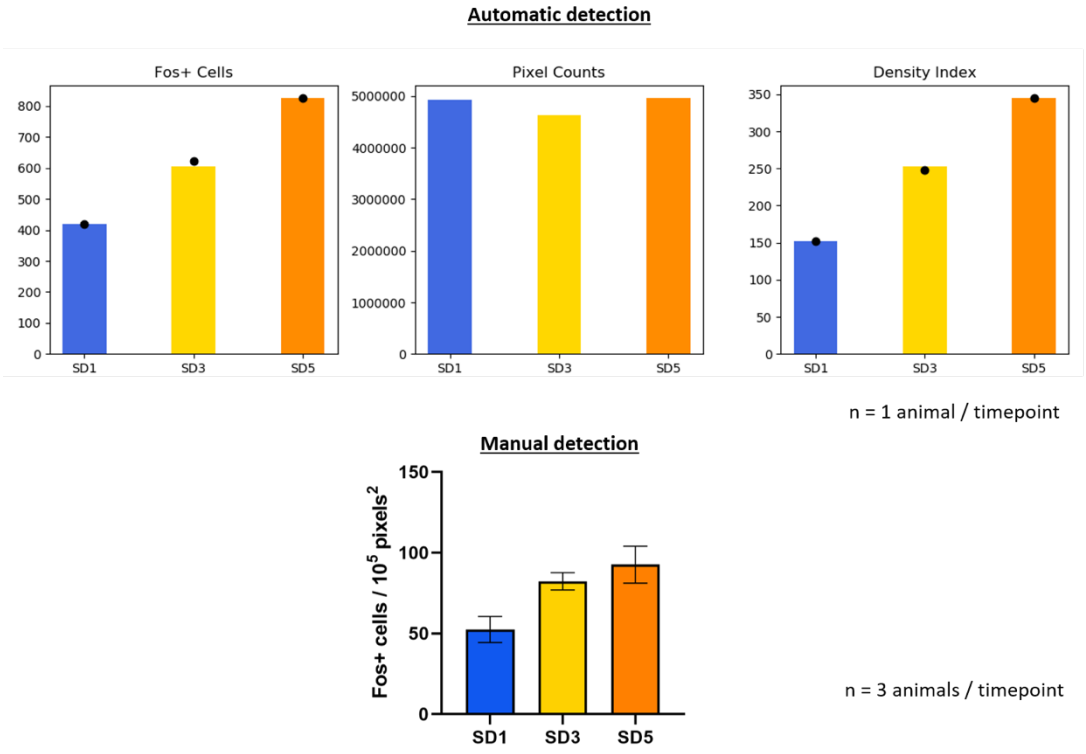

Figure 19: Automatic versus manual Fos+ cell count in CS.

Upper: Output from automated detection algorithm displaying Fos+ cell counts, pixel counts and density index for the Central Superior Raphe. Lower: Density index obtained through manual quantification of the same region.

Activity trends in the LHA were also validated. Automatically acquired data trends for this region suggest that neuronal activity increases over time, with the highest Fos+ cell count occurring in the SD3 timepoint (Fig. 20). A similar increase over time is also seen in the manual cell count data, with the SD3 timepoint having a higher cell count than would be expected if an exactly linear trend were followed. While absolute density index and Fos+ counts are higher overall in the 2D pipeline data than in the manually obtained data for both CS and LHA, the former is a more accurate estimate of overall activity due to the more objective nature of automatic cell detection.

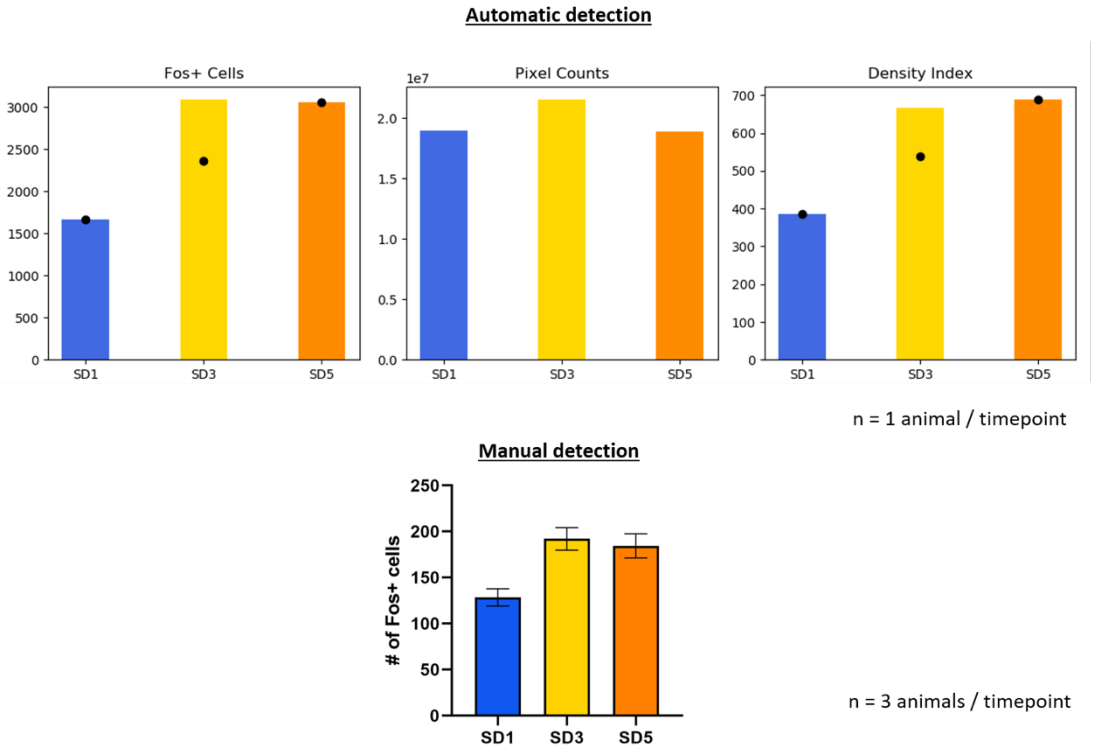

Figure 20: Automatic versus manual cell counts for LHA.
Upper: Output from automated detection algorithm displaying Fos+ cell counts, pixel counts and density index for the Lateral Hypothalamus. Lower: Density index obtained through manual quantification of the same region.

Chapter IV.

Discussion

Despite the fundamental nature of sleep, little is known about its function and regulation. Research has revealed that a complex network of neuronal populations work together to produce wake and sleep. How these regions are regulated, however, is a topic of much debate. Sleep deprivation is a commonly used tool to interrogate the function of the sleep homeostat. While often employed in the sleep field, less attention is paid to how different waking experiences during deprivation protocols can modulate sleep. Increasing evidence suggests that experiences during wake can differentially influence sleep EEG activity and architecture (Hung et al., 2013; Milinski et al., 2021). This study demonstrates that different methods of sleep deprivation result in differences in both wake and sleep EEG activity. Additionally, it was shown that the homeostat, while intact, works differently in the presence and absence of circadian rhythms.

It is well established that prolonged wakefulness results in an increase in delta and theta frequencies over time and that subsequent sleep results in a decrease in power within these frequency bands (Borbély, 1982; Vyazoskiy et a., 2011; Ehlen et al., 2013; Hung et al., 2013). Therefore, increases in delta and theta power have been used as an indirect measure of sleep pressure. Using linear discriminant analysis and density peak clustering, we classified wake into two distinct states based on whether the EEG signal exhibited high or low theta power, HWake and LWake, respectively. This is distinct from other definitions of wake which traditionally classify it as a single state. In this study, increases in delta and theta are seen in all deprivation methods in either HWake or

LWake (Fig. 11, 14). During SWS, there was a significant and reliable decrease in delta and theta power over time (Fig. 12, 14). These results are consistent with previous work demonstrating that delta and theta increase as a function of wake time and decrease during sleep.

Protocol-specific patterns in HWake can be seen in EEG activity for Misting, Flouring and Novel Objects (Fig. 11). A rise in the slope of the 2-8Hz HWake frequency band in Novel Objects was seen from early to late SD. Studies in humans and rodents have previously demonstrated that slow waves (1-4Hz) with a steeper slope are positively correlated with sleep pressure (Vyazoyskiy et al., 2007; Riedner et al., 2007; Kim et al., 2020). In rats, slow oscillations were found to have steep slopes at the beginning of the light phase or following sleep deprivation, when homeostatic sleep pressure is high. Slopes proceeded to decrease over time during sleep when sleep pressure and SWA decline (Vyazovskiy et al., 2007). The NO-specific signature seen from 2-8Hz is consistent with these reports and suggests that frequencies higher than 4Hz can also increase in slope in accordance with sleep pressure. It is important to note that this data was normalized by subtracting the minimal power seen per frequency bin, which may differ from traditional normalization methods.

Interestingly, changes in slow wave slope are used as measures of synaptic strength (Riedner et al., 2007). Evidence for the correlation between the two has been shown in both *in vitro* and *in vivo* studies demonstrating that long-term potentiation of synaptic transmission in the hippocampus and cortex results in an increase in the slope of postsynaptic potentials, while depression of this transmission results in a decrease in slope (Bliss et al., 1973; Timofeev et al., 2000; Vyazocskiy et al., 2007). It is possible

that an increased slope in 2-8Hz is a signature of NO, specifically, because mice in this deprivation engage in exploratory behavior, resulting in an increase in synaptic strength as information is collected about their environment. This results in an increase in sleep pressure, or Process S, which is then dissipated during recovery sleep. This theory is compatible with the synaptic homeostasis model which states that, as synaptic strength increases over the course of the day, synaptic transmission is returned to baseline over the course of ensuing sleep.

Another protocol-specific pattern seen in HWake is a distinct peak in the 2-8Hz range present in both Misting and Flouring (Fig. 11). Because these deprivations are similar in terms of the response generated by the stimulus (grooming versus exploration), the specificity of this signal suggests that it is a result of the type of deprivation administered. While Novel Objects and Burrowing are designed to engage mice in more physically and mentally active innate behavior such as exploration and burrowing, Misting and Flouring engage mice in grooming behavior only. Between these deprivations, Misting resulted in a higher peak in this range than Flouring. This could be a product of multiple factors. Mice made more sleep attempts in Flouring and appeared less bothered by the "puff" of flour than they did with water spritzes, ultimately engaging in less grooming and proving it to be a less effective sleep deprivation method (Fig. 9). Therefore, floured mice likely built up less sleep pressure compared to misted ones. This could explain the lower peak in the 2-8Hz range for Flouring relative to Misting. It is also possible that the water droplets in Misting activated the cortex more than the fine powder in Flouring, resulting in a higher cortical EEG signal. The higher peak in the EEG could

be due to increased thalamic and cortical activity for the above-mentioned reasons or perhaps a reflection of the mice's annoyance with the stimulus over time.

When plotted in state space, it was clear a representative mouse spent more time in LWake during the Misting and Flouring protocols than in Burrowing or NO (Fig. 10). It also made many more transitions into SWS, a nice visualization of the same data reflected for the whole group in the quantification of sleep attempts per deprivation method (Figure 9). Notably, the mouse spent the least amount of time in LWake during NO, followed by Burrowing. This can also be seen in Figure 16 for B6 mice.

With regard to sleep, all deprivation methods resulted in a decrease in delta and theta power over the course of SD (Fig. 14). Misting appears to result in the highest amount of SWS during RS, followed by Burrowing and then NO. It is likely that the high delta peak seen in Misting relative to the other two protocols reflects higher sleep pressure in this deprivation due to a lack of engagement during the protocol itself and results in a greater amount of SWS during the recovery period. This might explain why NO results in the least amount of SWS. If true, this provides evidence that experiences during wake differentially modulate the amount of subsequent SWS. Together, data from the comparison of different deprivation methods on wake and sleep adds to previously published work suggesting that waking experience interacts with the sleep homeostat to produce differences in sleep.

According to Borbély's two process model, homeostatic and circadian processes interact to regulate sleep, but are distinct from one another. This has been demonstrated in studies showing that animals rendered arrhythmic by lesions to the SCN did not have disrupted sleep homeostasis (Toblet et al., 1983; Trachsel et al., 1992). While many

studies have used clock gene knockouts to investigate how a lack of circadian rhythms influences sleep, these studies use mice in which clock genes are deleted from every cell in the body. This often results in reduced viability and survival rates and could potentially produce confounding factors (Lee et al., 2005). The current study utilizes Nms-iCre(+/-); Bmal1(fl/fl) mice which have the Bmal1 gene knocked out in a particular subset of neurons in the SCN, leading to the abolishment of circadian locomotor activity. Accordingly, Nms mice lack consolidated periods of wake and sleep unlike wildtype controls (Lee et al., 2015).

In this study, I compared the electrophysiological activity of Nms and B6 mice to determine differences in state distribution at baseline and during and after SD. Sleep architecture was also examined. When compared at baseline, the state distribution of rhythmic and arrhythmic animals was found to be fundamentally different (Fig. 15). Notably, Nms mice spend significantly more time in LWake and SWS compared to B6 mice. This may reflect the fact that arrhythmic animals have less consolidated wake and perhaps have lower arousal throughout the day compared to rhythmic animals, explaining why they spend more time in SWS. A 2017 study by Ehlen et al. found a similar increase in baseline NREM sleep in a whole-body Bmal1 knockout mouse. They demonstrated, however, that the rescue of Bmal1 expression in skeletal muscle re-established wild type levels of baseline NREM sleep (Ehlen et al., 2017). Ehlen et al. conclude that skeletal muscle expression is both necessary and sufficient to regulate total sleep amounts. Interestingly, this differs from what is seen in the mice used in this study. The mice I used lack Bmal1 expression in a subset of neurons in the SCN which express neuromedin-S, while whole-body levels remain unaffected. The fact that SWS levels

remained higher in these animals than wild type levels despite Bmal1 expression in skeletal muscles suggests that these muscles may not be sufficient to regulate sleep amounts.

During Misting, Nms mice spent an increased amount of time in LWake and less time in SWS relative to B6 mice (Fig. 16). This is notable because differences in the percent of time spent in these states were not seen in other deprivation methods. This could be explained by the fact that mice are more actively engaged during Burrowing and NO. Therefore, all mice experience greater arousal and spend more time in HWake (Figure 16). Because mice experience lower arousal in Misting, the percent of time in LWake more closely resembles the pattern seen at baseline for each strain (Fig. 15, 16). The increased percent of time spent in SWS following SD can be explained by the fact that rhythmic mice experience consolidated periods of wake (Fig. 16). Because rhythmic mice were at the end of their active period at the start of deprivation, they had accumulated a high amount of sleep pressure. Therefore, it makes sense that they would spend a greater percentage of time in SWS following Misting than arrhythmic mice and display higher cumulative amounts of SWS (Fig. 17A, B). A significant increase in REM sleep for B6 mice relative their Nms counterparts was seen in Burrowing. It is possible that this increase is also due to rhythmic animals' lack of consolidated sleep and perhaps a compensation for high physical activity. Surprisingly, Nms mice spend approximately half the time in REM sleep following deprivation than B6 (Fig 17B, D). The reason for this difference is unclear and necessitates more research to understand why REM sleep levels are so low for Nms mice during recovery, especially when they spend a similar percentage of time in REM at baseline as B6 animals.

Aside from EEG activity, another important aspect of understanding the sleep homeostat is investigating how different brain regions contribute to this regulation. Many studies focus on cell activity in a given brain region; however, a full interrogation of sleep-wake circuitry requires a whole brain approach. While there are software packages developed to quantify whole brain neuronal activity, they often run into trouble finding landmark correspondences between references atlases and sample images, making it difficult to get an accurate quantification of cell activity. Because of this, I helped develop a pipeline to automatically detect brain-wide neuronal activity using ImageJ and custom Python scripts, allowing for increased adaptability in warping reference atlases to 2D section data. Expression of the immediate early gene *c-fos* is a well-established marker of neuronal activity (Chung, 2015). Therefore, this pipeline was designed to take an input of 2D images stained for *c-fos* expression. It can also be adapted for use with other markers of activity such as phospho-S6 (pS6).

There are multiple directions for further investigation. Looking at how EEG activity changes per hour during SD and RS and how long the effects of waking experience last following SD are of great interest. The latter could be accomplished by extending analysis by an additional 24 hours past the end of SD. This should be done for both rhythmic and arrhythmic animals to further dissect the circadian component of sleep regulation. Sleep deprivation could also be performed at the start of the dark period and state dynamics compared to those obtained at lights on. Another potential avenue of exploration would be to see whether brain regions are differentially activated or inhibited during and after each deprivation protocol. Common trends in regions previously implicated in sleep-wake production and/or regulation among the protocols may point to

commonly shared regulatory areas, while varying regional activity could suggest how different wake experiences lead to differences in sleep-wake regulation.

It is widely accepted that prolonged wakefulness results in the accumulation of sleep pressure which dissipates over the course of sleep. The sleep homeostat is thought to be regulated by two processes, homeostatic and circadian, that interact in a complex way to integrate prior wake and circadian time. Understanding how each contributes to the regulation of sleep and wake states necessitates a multi-pronged approach, including the analysis of EEG activity and brain-wide neuronal activity. In this study, I demonstrated that prior wake experience during sleep deprivation not only changes sleep state dynamics and total amounts but also results in protocol-specific EEG patterns. Differences in sleep and wake regulation was shown to be different in the presence and absence of circadian rhythms, as reflected in the percent of time spent in each sleep and wake states at baseline and during and after sleep deprivation.

References

Abrams, J. K., Johnson, P. L., Hollis, J. H., & Lowry, C. A. (2004). Anatomic and Functional Topography of the Dorsal Raphe Nucleus. *Annals of the New York Academy of Sciences*, *1018*(1), 46–57. doi: 10.1196/annals.1296.005

Achermann, Peter. (2009). EEG Analysis Applied to Sleep. Epileptologie. 26. 10.5167/uzh-19935.

Adamantidis, A. R., Gutierrez Herrera, C., & Gent, T. C. (2019). Oscillating circuitries in the sleeping brain. Nature reviews. Neuroscience, 20(12), 746–762. https://doi.org/10.1038/s41583-019-0223-4

Arpa, J., Padrino, C., Rodriguez-Albarino, A., & Andres, I. D. (1998). Centralis superior raphe, reticularis pontis nuclei, and sleep-wakefulness cycle in cats. Journal of Sleep Research, 7(4), 263–275. doi: 10.1046/j.1365-2869.1998.00124.x

Bliss, T. V., & Lomo, T. (1973). Long-lasting potentiation of synaptic transmission in the dentate area of the anaesthetized rabbit following stimulation of the perforant path. The Journal of physiology, 232(2), 331–356. https://doi.org/10.1113/jphysiol.1973.sp010273

Borbély A. A. (1982). A two process model of sleep regulation. Human neurobiology, 1(3), 195–204.

Borbély, A. A., Daan, S., Wirz-Justice, A., & Deboer, T. (2016). The two-process model of sleep regulation: a reappraisal. Journal of Sleep Research, 25(2), 131–143. doi: 10.1111/jsr.12371

Boucetta, S., Cisse, Y., Mainville, L., Morales, M., & Jones, B. E. (2014). Discharge Profiles across the Sleep-Waking Cycle of Identified Cholinergic, GABAergic, and Glutamatergic Neurons in the Pontomesencephalic Tegmentum of the Rat. Journal of Neuroscience, 34(13), 4708–4727. doi: 10.1523/jneurosci.2617-13.2014

Buhot, M.-C. (1997). Serotonin receptors in cognitive behaviors. Current Opinion in Neurobiology, 7(2), 243–254. doi: 10.1016/s0959-4388(97)80013-x

Cardin J. A. (2016). Snapshots of the Brain in Action: Local Circuit Operations through the Lens of γ Oscillations. The Journal of neuroscience : the official journal of the Society for Neuroscience, 36(41), 10496–10504. https://doi.org/10.1523/JNEUROSCI.1021-16.2016

Cirelli, C., Pompeiano, M., & Tononi, G. (1996). Neuronal gene expression in the waking state: a role for the locus coeruleus. Science (New York, N.Y.), 274(5290), 1211–1215. https://doi.org/10.1126/science.274.5290.1211

Cirelli, C., Gutierrez, C. M., & Tononi, G. (2004). Extensive and Divergent Effects of Sleep and Wakefulness on Brain Gene Expression. Neuron, 41(1), 35–43. https://doi.org/10.1016/s0896-6273(03)00814-6

Cirelli, C., Huber, R., Gopalakrishnan, A., Southard, T. L., & Tononi, G. (2005). Locus ceruleus control of slow-wave homeostasis. The Journal of neuroscience : the official journal of the Society for Neuroscience, 25(18), 4503–4511. https://doi.org/10.1523/JNEUROSCI.4845-04.2005

Chou, T. C., Scammell, T. E., Gooley, J. J., Gaus, S. E., Saper, C. B., & Lu, J. (2003). Critical Role of Dorsomedial Hypothalamic Nucleus in a Wide Range of Behavioral Circadian Rhythms. The Journal of Neuroscience, 23(33), 10691–10702. doi: 10.1523/jneurosci.23-33-10691.2003

Chung L. (2015). A Brief Introduction to the Transduction of Neural Activity into Fos Signal. Development & reproduction, 19(2), 61–67. https://doi.org/10.12717/DR.2015.19.2.061

Colavito, V., Fabene, P. F., Grassi-Zucconi, G., Pifferi, F., Lamberty, Y., Bentivoglio, M., & Bertini, G. (2013). Experimental sleep deprivation as a tool to test memory deficits in rodents. Frontiers in systems neuroscience, 7, 106. https://doi.org/10.3389/fnsys.2013.00106

Deboer, T. (2018). Sleep homeostasis and the circadian clock: Do the circadian pacemaker and the sleep homeostat influence each other's functioning? Neurobiology of Sleep and Circadian Rhythms, 5, 68–77. doi: 10.1016/j.nbscr.2018.02.003

Descarries, L., Watkins, K. C., Garcia, S., & Beaudet, A. (1982). The serotonin neurons in nucleus raphe dorsalis of adult rat: A light and electron microscope radioautographic study. The Journal of Comparative Neurology, 207(3), 239–254. doi: 10.1002/cne.902070305

Eastman, C. I., Mistlberger, R. E., & Rechtschaffen, A. (1984). Suprachiasmatic nuclei lesions eliminate circadian temperature and sleep rhythms in the rat. Physiology & Behavior, 32(3), 357–368. doi: 10.1016/0031-9384(84)90248-8

Ehlen, J. C., Jefferson, F., Brager, A. J., Benveniste, M., & Paul, K. N. (2013). Period-amplitude analysis reveals wake-dependent changes in the electroencephalogram during sleep deprivation. Sleep, 36(11), 1723–1735. https://doi.org/10.5665/sleep.3138

Feld, G. B., & Born, J. (2017). Sculpting memory during sleep: concurrent consolidation and forgetting. Current Opinion in Neurobiology, 44, 20–27. doi: 10.1016/j.conb.2017.02.012

Finelli, L. A., Baumann, H., Borbély, A. A., & Achermann, P. (2000). Dual electroencephalogram markers of human sleep homeostasis: correlation between theta activity in waking and slow-wave activity in sleep. Neuroscience, 101(3), 523–529. https://doi.org/10.1016/s0306-4522(00)00409-7

Fu, W., Maître, E. L., Fabre, V., Bernard, J.-F., Xu, Z.-Q. D., & Hökfelt, T. (2010). Chemical neuroanatomy of the dorsal raphe nucleus and adjacent structures of the mouse brain. The Journal of Comparative Neurology, 518(17), 3464–3494. doi: 10.1002/cne.22407

Fuller, P. M., Gooley, J. J., & Saper, C. B. (2006). Neurobiology of the Sleep-Wake Cycle: Sleep Architecture, Circadian Regulation, and Regulatory Feedback. Journal of Biological Rhythms, 21(6), 482–493. doi: 10.1177/0748730406294627

Fuller, P., Sherman, D., Pedersen, N. P., Saper, C. B., & Lu, J. (2011). Reassessment of the structural basis of the ascending arousal system. The Journal of Comparative Neurology, 519(5), 933–956. doi: 10.1002/cne.22559

Gross, D. W., & Gotman, J. (1999). Correlation of high-frequency oscillations with the sleep-wake cycle and cognitive activity in humans. Neuroscience, 94(4), 1005–1018. https://doi.org/10.1016/s0306-4522(99)00343-7

Hairston IS, Little MT, Scanlon MD, Barakat MT, Palmer TD, Sapolsky RM, Heller HC. Sleep restriction suppresses neurogenesis induced by hippocampus-dependent learning. J Neurophysiol. 2005 Dec;94(6):4224-33. doi: 10.1152/jn.00218.2005. Epub 2005 Jul 13. PMID: 16014798.

Hung, C. S., Sarasso, S., Ferrarelli, F., Riedner, B., Ghilardi, M. F., Cirelli, C., & Tononi, G. (2013). Local experience-dependent changes in the wake EEG after prolonged wakefulness. Sleep, 36(1), 59–72. https://doi.org/10.5665/sleep.2302

Irwin, M. R., & Opp, M. R. (2016). Sleep Health: Reciprocal Regulation of Sleep and Innate Immunity. Neuropsychopharmacology, 42(1), 129–155. doi: 10.1038/npp.2016.148

Jacobs, B. L., & Azmitia, E. C. (1992). Structure and function of the brain serotonin system. Physiological Reviews, 72(1), 165–229. doi: 10.1152/physrev.1992.72.1.165

Katsageorgiou, V.-M., Sona, D., Zanotto, M., Lassi, G., Garcia-Garcia, C., Tucci, V., & Murino, V. (2018). A novel unsupervised analysis of electrophysiological signals reveals new sleep substages in mice. PLOS Biology, 16(5). doi: 10.1371/journal.pbio.2003663

Kim, B., Hwang, E., Strecker, R. E., Choi, J. H., & Kim, Y. (2020). Differential modulation of NREM sleep regulation and EEG topography by chronic sleep restriction in mice. Scientific Reports, 10(1). https://doi.org/10.1038/s41598-019-54790-y

Krueger, J. M. et al. (2019) ‘Local sleep’, Sleep Medicine Reviews, 43, pp. 14–21. doi: 10.1016/j.smrv.2018.10.001.

Lack, L. C., Gradisar, M., Someren, E. J. V., Wright, H. R., & Lushington, K. (2008). The relationship between insomnia and body temperatures. Sleep Medicine Reviews, 12(4), 307–317. doi: 10.1016/j.smrv.2008.02.003

Lee, I. T., Chang, A. S., Manandhar, M., Shan, Y., Fan, J., Izumo, M., … Yanagisawa, M. (2015). Neuromedin S-Producing Neurons Act as Essential Pacemakers in the Suprachiasmatic Nucleus to Couple Clock Neurons and Dictate Circadian Rhythms. Neuron, 85(5), 1086–1102. doi: 10.1016/j.neuron.2015.02.006

Lowry, C. A., Hale, M. W., Evans, A. K., Heerkens, J., Staub, D. R., Gasser, P. J., & Shekhar, A. (2008). Serotonergic systems, anxiety, and affective disorder: focus on the dorsomedial part of the dorsal raphe nucleus. Annals of the New York Academy of Sciences, 1148, 86–94. doi: 10.1196/annals.1410.004

Lu, J., Zhang, Y.-H., Chou, T. C., Gaus, S. E., Elmquist, J. K., Shiromani, P., & Saper, C. B. (2001). Contrasting Effects of Ibotenate Lesions of the Paraventricular Nucleus and Subparaventricular Zone on Sleep–Wake Cycle and Temperature Regulation. The Journal of Neuroscience, 21(13), 4864–4874. doi: 10.1523/jneurosci.21-13-04864.2001

López, J. F., Akil, H., & Watson, S. J. (1999). Neural circuits mediating stress. Biological Psychiatry, 46(11), 1461–1471. doi: 10.1016/s0006-3223(99)00266-8

Milinski, L., Fisher, S. P., Cui, N., McKillop, L. E., Blanco-Duque, C., Ang, G., Yamagata, T., Bannerman, D. M., & Vyazovskiy, V. V. (2021). Waking experience modulates sleep need in mice. BMC biology, 19(1), 65. https://doi.org/10.1186/s12915-021-00982-w

Miyazaki, S., Liu, C.-Y., & Hayashi, Y. (2017). Sleep in vertebrate and invertebrate animals, and insights into the function and evolution of sleep. Neuroscience Research, 118, 3–12. doi: 10.1016/j.neures.2017.04.017

Naylor, E., Bergmann, B. M., Krauski, K., Zee, P. C., Takahashi, J. S., Vitaterna, M. H., & Turek, F. W. (2000). The circadian clock mutation alters sleep homeostasis in the mouse. The Journal of neuroscience : the official journal of the Society for Neuroscience, 20(21), 8138–8143. https://doi.org/10.1523/JNEUROSCI.20-21-08138.2000

Pollak Dorocic, I., Fürth, D., Xuan, Y., Johansson, Y., Pozzi, L., Silberberg, G., … Meletis, K. (2014). A Whole-Brain Atlas of Inputs to Serotonergic Neurons of the Dorsal and Median Raphe Nuclei. Neuron, 83(3), 663–678. doi: 10.1016/j.neuron.2014.07.002

Qing-Ping, W., & Nakai, Y. (1994). The dorsal raphe: An important nucleus in pain modulation. Brain Research Bulletin, 34(6), 575–585. doi: 10.1016/0361-9230(94)90143-0

Ranson, S. W. (1939). Somnolence Caused By Hypothalamic Lesions In The Monkey. Archives of Neurology And Psychiatry, 41(1), 1. doi: 10.1001/archneurpsyc.1939.02270130011001

Ren, J., Isakova, A., Friedmann, D., Zeng, J., Grutzner, S. M., Pun, A., … Luo, L. (2019). Author response: Single-cell transcriptomes and whole-brain projections of serotonin neurons in the mouse dorsal and median raphe nuclei. ELife, 1–36. doi: 10.7554/elife.49424.043

Riedner, B. A., Vyazovskiy, V. V., Huber, R., Massimini, M., Esser, S., Murphy, M., & Tononi, G. (2007). Sleep homeostasis and cortical synchronization: III. A high-density EEG study of sleep slow waves in humans. Sleep, 30(12), 1643–1657. https://doi.org/10.1093/sleep/30.12.1643

Saper, C. B., & Fuller, P. M. (2017). Wake–sleep circuitry: an overview. Current Opinion in Neurobiology, 44, 186–192. doi: 10.1016/j.conb.2017.03.021

Scammell, T. E., Arrigoni, E., & Lipton, J. O. (2017). Neural Circuitry of Wakefulness and Sleep. Neuron, 93(4), 747–765. doi: 10.1016/j.neuron.2017.01.014

Shaw, P. J., Tononi, G., Greenspan, R. J., & Robinson, D. F. (2002). Stress response genes protect against lethal effects of sleep deprivation in Drosophila. Nature, 417(6886), 287–291. https://doi.org/10.1038/417287a

Shiromani, P. J., Xu, M., Winston, E. M., Shiromani, S. N., Gerashchenko, D., & Weaver, D. R. (2004). Sleep rhythmicity and homeostasis in mice with targeted disruption of mPeriod genes. American journal of physiology. Regulatory, integrative and comparative physiology, 287(1), R47–R57. https://doi.org/10.1152/ajpregu.00138.2004

Siclari, F., Bernardi, G., Cataldi, J., & Tononi, G. (2018). Dreaming in NREM Sleep: A High-Density EEG Study of Slow Waves and Spindles. The Journal of neuroscience : the official journal of the Society for Neuroscience, 38(43), 9175–9185. https://doi.org/10.1523/JNEUROSCI.0855-18.2018

Steinbusch, H., Kooy, D. V. D., Verhofstad, A., & Pellegrino, A. (1980). Serotonergic and non-serotonergic projections from the nucleus raphe dorsalis to the caudate-putamen complex in the rat, studied by a combined immunofluorescence and fluorescent retrograde axonal labeling technique. Neuroscience Letters, 19(2), 137–142. doi: 10.1016/0304-3940(80)90184-6

Timofeev, I., Grenier, F., Bazhenov, M., Sejnowski, T. J., & Steriade, M. (2000). Origin of slow cortical oscillations in deafferented cortical slabs. Cerebral cortex (New York, N.Y.: 1991), 10(12), 1185–1199. https://doi.org/10.1093/cercor/10.12.1185

Tobler, I., Borbély, A., & Groos, G. (1983). The effect of sleep deprivation on sleep in rats with suprachiasmatic lesions. Neuroscience Letters, 42(1), 49–54. doi: 10.1016/0304-3940(83)90420-2

Tononi, G., & Cirelli, C. (2006). Sleep function and synaptic homeostasis. Sleep medicine reviews, 10(1), 49–62. https://doi.org/10.1016/j.smrv.2005.05.002

Trachsel, L., Edgar, D. M., Seidel, W. F., & Heller, H. C. (1992). Sleep homeostasis in suprachiasmatic nuclei-lesioned rats: effects of sleep deprivation and triazolam administration. Brain Research, 589(2), 253–261. doi: 10.1016/0006-8993(92)91284-l

Vyazovskiy, V. V., Riedner, B. A., Cirelli, C., & Tononi, G. (2007). Sleep homeostasis and cortical synchronization: II. A local field potential study of sleep slow waves in the rat. Sleep, 30(12), 1631–1642. https://doi.org/10.1093/sleep/30.12.1631

Vyazovskiy, V. V., Olcese, U., Hanlon, E. C., Nir, Y., Cirelli, C., & Tononi, G. (2011). Local sleep in awake rats. Nature, 472(7344), 443–447. https://doi.org/10.1038/nature10009

Weber, F., & Dan, Y. (2016). Circuit-based interrogation of sleep control. Nature, 538(7623), 51–59. doi: 10.1038/nature19773

Wisor, J. P., O'Hara, B. F., Terao, A., Selby, C. P., Kilduff, T. S., Sancar, A., Edgar, D. M., & Franken, P. (2002). A role for cryptochromes in sleep regulation. BMC neuroscience, 3, 20. https://doi.org/10.1186/1471-2202-3-20

Zimmerman, J. E., Naidoo, N., Raizen, D. M., & Pack, A. I. (2008). Conservation of sleep: insights from non-mammalian model systems. Trends in Neurosciences, 31(7), 371–376. doi: 10.1016/j.tins.2008.05.001